


RESEARCH

Open Access



SNCA genetic lowering reveals differential cognitive function of alpha-synuclein dependent on sex

Jennifer L. Brown^{1,2,4}, Damyan W. Hart^{2,4}, Gabriel E. Boyle^{2,4,7}, Taylor G. Brown^{2,3,4}, Michael LaCroix^{2,4,6}, Andrés M. Baraibar^{2,8}, Ross Pelzel^{1,2,4}, Minwoo Kim^{2,4}, Mathew A. Sherman^{2,4}, Samuel Boes^{2,4}, Michelle Sung^{2,4,9}, Tracy Cole^{5,10}, Michael K. Lee^{2,4}, Alfonso Araque^{1,2} and Sylvain E. Lesné^{1,2,4*} 

Abstract

Antisense oligonucleotide (ASO) therapy for neurological disease has been successful in clinical settings and its potential has generated hope for Alzheimer's disease (AD). We previously described that ablating *SNCA* encoding for α -synuclein (α Syn) in a mouse model of AD was beneficial. Here, we sought to demonstrate whether transient reduction of α Syn expression using ASO^{SNCA} could be therapeutic in a mouse model of AD. The efficacy of the ASO^{SNCA} was measured via immunocytochemistry, RT-qPCR and western blotting. To assess spatial learning and memory, ASO^{SNCA} or PBS-injected APP and non-transgenic (NTG) mice, and separate groups of *SNCA*-null mice, were tested on the Barnes circular maze. Hippocampal slice electrophysiology and transcriptomic profiling were used to explore synaptic function and differential gene expression between groups. Reduction of *SNCA* transcripts alleviated cognitive deficits in male transgenic animals, but surprisingly, not in females. To determine the functional cause of this differential effect, we assessed memory function in *SNCA*-null mice. Learning and memory were intact in male mice but impaired in female animals, revealing that the role of α Syn on cognitive function is sex-specific. Transcriptional analyses identified a differentially expressed gene network centered around *EGR1*, a central modulator of learning and memory, in the hippocampi of *SNCA*-null mice. Thus, these novel results demonstrate that the function of α Syn on memory differs between male and female brains.

Keywords Alpha-synuclein, Spatial memory, Sex, Antisense oligonucleotide, Synucleinopathy, Alzheimer's disease, Early growth response 1

*Correspondence:

Sylvain E. Lesné
lesne002@umn.edu

¹ Graduate Program in Neuroscience, University of Minnesota, Minneapolis, MN, USA

² Department of Neuroscience, University of Minnesota, Minneapolis, MN, USA

³ Medical Scientist Training Program, University of Minnesota, Minneapolis, MN, USA

⁴ Institute for Translational Neuroscience, University of Minnesota, Wallin Medical Biosciences Building (Room 4-114), 2101 Sixth Street SE, CDC 2641, Minneapolis, MN 55414, USA

⁵ Ionis Pharmaceuticals Inc., Carlsbad, CA, USA

⁶ Present Address: Medical Scientist Training Program, University of Texas Southwestern Medical School, Dallas, TX 75390, USA

⁷ Present Address: Graduate Program in Molecular and Cellular Biology, University of Washington, Seattle, WA 98195, USA

⁸ Present Address: Department of Neurosciences, University of the Basque Country UPV/EHU, Leioa, Spain

⁹ Present Address: Bloomberg School of Public Health, Johns Hopkins University, Baltimore, MD 21218, USA

¹⁰ Present Address: n-Lorem Foundation, Carlsbad, CA 92010, USA



© The Author(s) 2022, corrected publication 2024. **Open Access** This article is licensed under a Creative Commons Attribution 4.0 International License, which permits use, sharing, adaptation, distribution and reproduction in any medium or format, as long as you give appropriate credit to the original author(s) and the source, provide a link to the Creative Commons licence, and indicate if changes were made. The images or other third party material in this article are included in the article's Creative Commons licence, unless indicated otherwise in a credit line to the material. If material is not included in the article's Creative Commons licence and your intended use is not permitted by statutory regulation or exceeds the permitted use, you will need to obtain permission directly from the copyright holder. To view a copy of this licence, visit <http://creativecommons.org/licenses/by/4.0/>. The Creative Commons Public Domain Dedication waiver (<http://creativecommons.org/publicdomain/zero/1.0/>) applies to the data made available in this article, unless otherwise stated in a credit line to the data.

Introduction

The number of people suffering from Alzheimer's disease (AD) continues to grow, and the treatment options remain few. AD is a progressive neurodegenerative disease characterized by a loss of cognitive function, including reasoning and memory. The hallmarks of AD, tau neurofibrillary tangles and amyloid-beta (A β) plaques, are rarely seen in isolation. Over 50% of AD brains also display Lewy bodies, composed of aggregated alpha-synuclein (α Syn), which are classically linked to Parkinson's disease [48, 52]. While the appearance of mixed proteinopathies is now more commonly recognized in the aging brain [8], accumulating evidence suggests a link between α Syn and AD [25, 29, 30, 38].

Transgenic mouse models have been used to investigate the potential contribution of α Syn to AD phenotypes but these studies have often resulted in diverging conclusions [3, 11, 35, 49, 56]. Using a bidirectional approach in a controlled genetic background, data from our lab showed that male α Syn knock-out mice overexpressing human mutant amyloid precursor protein (APP) displayed improved spatial reference memory and survival but increased A β deposition [25]. Conversely, male mice overexpressing human wild-type α Syn and APP presented with an exacerbated cognitive deficit accompanied by a decrease in A β plaques [25]. These results indicated that α Syn is a profound modulator of AD phenotypes in male APP mice. Consequently, evidence in both humans and mice suggests that decreasing α Syn might be beneficial in AD.

Because our past work utilized a genetic approach rather than a method suitable for the clinic, we initially aimed to investigate the use of α Syn-lowering antisense oligonucleotides as a possible translational therapy for AD. Briefly, antisense oligonucleotides (ASOs) are short, single-stranded DNA sequences which can be utilized to reduce the expression of target gene mRNA and protein in many human disease models [27, 47], including AD [14]. The Food and Drug Administration has approved Spinraza[®] (Nusinersen), an ASO therapy for adults and infants suffering from spinal muscular atrophy, demonstrating that ASOs can be safe and effective treatments for some neurological disorders [5]. Consequently, the interest in ASO-mediated translational approaches has skyrocketed in this field [47] and generated hope in patients and their families.

In this study, we first used a single injection of an ASO targeting mouse *SNCA* (ASO^{SNCA}), the gene that encodes α Syn, to reduce α Syn mRNA and protein in a well-known APP transgenic mouse model of AD and non-transgenic (NTG) littermates. While the male APP mice treated with the ASO^{SNCA} showed cognitive improvements, both APP and NTG female mice unexpectedly performed

worse. To determine the functional cause of this sex-specific effect, we performed behavioral and transcriptional analyses using α Syn knockout (α Syn-KO) mice. Learning and memory studies revealed that *SNCA* gene deletion caused a cognitive delay in female animals only. Transcriptomic profiling identified a gene network centered around *EGR1*, a key transcription factor involved in learning and memory [24, 60], that was differentially expressed across sex in the hippocampi of α Syn-KO mice. Finally, we confirmed sex-dependent changes in *Egr1* protein expression in hippocampal neurons from α Syn-KO mice. To our knowledge, these results are the first to reveal a sex-specific role of α Syn on cognitive function and transcriptional responses.

Materials and methods

Animals

Two genetically-modified lines were used: (i) *SNCA*-null mice [1] and (iii) J20 APP (originally called hAPPJ20) mice [39]. *SNCA*-null mice were obtained from Jackson laboratories and backcrossed to C57BL6/J for greater than 10 generations. Every 6 months, the homozygous KO mice are outbred to wild-type C57BL6/J and homozygous KO mice are reconstituted from the mating of heterozygous animals. Both male and female animals were used in equal numbers for biochemical studies and Barnes maze behavioral testing. All animal procedures and studies were reviewed and approved by the University of Minnesota Institutional Animal Care and Use Committee and Institutional Review Board and the animals' care was in accordance with institutional guidelines.

Antisense oligonucleotides

The synthesis and purification of all lyophilized ASOs was formulated in PBS as previously described [12] and stored at -20°C (kind gifts from Drs. Tracy Cole and Holly Kordasiewicz, Ionis Pharmaceuticals Inc., Carlsbad, CA, USA). The sequences for ASO1 and ASO2 (5'-3') are TTTAATTACTTCCACCA and CTGTAAAGT CACAAGCA respectively. The ASOs contain modified nucleotides, including 2'-O-methoxyethylribose (MOE) and (S)-2',4'-constrained 2'-O-ethyl (cEt) 2'-O-methoxyethyl modifications, as well as phosphorothioate backbone modifications.

Primary neurons

Primary neuron cultures were prepared as previously described [40, 54].

Protein extractions

Soluble aggregation-prone protein levels in brain tissue were analyzed using the extraction protocol previously

described [32], with a detailed 32-step-protocol explained in the latter. The goal of this lysis process is to fractionate proteins based on their cellular compartmentalization. The sequential separation allows the recovery of a predicted protein in its compartment of 75–90% as previously described [30, 32]. Briefly, dissected frozen hemiforebrain tissues (125–200 mg) are gently dissociated in NP40-lysis buffer (50 mM Tris–HCl [pH 7.6], 0.01% NP-40, 150 mM NaCl, 2 mM EDTA, 0.1% SDS) and centrifuged at 800×g, to separate extracellular proteins contained in the supernatant. The remaining loose pellet is then lysed with TNT-lysis buffer (50 mM Tris–HCl, pH 7.4, 150 mM NaCl, 0.1% Triton X-100), and centrifuged at 16,100×g, to separate intracellular proteins present in the aqueous phase. The subsequent pellet is finally dissociated in RIPA-lysis buffer (50 mM Tris–HCl, pH 7.4, 150 mM NaCl, 0.5% Triton X-100, 1 mM EDTA, 3% SDS, 1% deoxycholate) and centrifuged at 16,100×g, to separate membrane-bound proteins present in the supernatant. All supernatants were ultra-centrifuged for 20 min at 100,000×g. Before analysis, fractions were depleted of endogenous immunoglobulins by incubating lysates with 50 µL of Protein A-Sepharose, Fast Flow® beads for one hour at 4 °C, followed by 50 µL of Protein G-Sepharose, Fast Flow® beads (GE Healthcare Life Sciences). Protein amounts were determined with the Bicinchoninic acid protein assay (BCA Protein Assay, Pierce™).

Antibodies

The following primary antibodies were used in this study: 6E10 [1:2,000] (Catalog no. SIG-803003, BioLegend), 4D6 anti- α -Synuclein [1:500–10,000] (Catalog no. SIG-39725, BioLegend), anti- β -Synuclein [1:5000] (Catalog no. ab76111, Abcam), anti-ASO (gift from Dr. Tracy Cole at Ionis Pharmaceuticals Inc.) [1:10,000], anti-NeuN [1:500] (Catalog no. ABU78, EMD Millipore), anti-Egr1 [1:100] (Catalog no. 22008-1-AP, Proteintech). The following secondary antibodies were used in this study: Alexa Fluor™ (Molecular Probes, Invitrogen) Goat-anti-Chicken 488 (Catalog no. A-11039), 568 (Catalog no. A-11041), 647 (Catalog no. A-21449), Goat-anti-Mouse 568 (Catalog no. A-11004), 647 (Catalog no. A-21235), Goat-anti-Rabbit 488 (Catalog no. A-11034), 555 (Catalog no. A-21435), 568 (Catalog no. A-11036), DyLight® Goat-anti-Mouse 405 (Catalog no. 35501BID), IRDye® (Li-COR) 800cw Goat anti-Rabbit (Catalog no. 925–32,211), IRDye® (Li-COR) 680LT Goat anti-Mouse (Catalog no. 925-68020).

Egr1 immunofluorochemistry and spot analysis

30 µm mouse brain sections were prepared using a vibratome (Leica) and stained with anti-Egr1 (Proteintech, Catalog no. 22008-1-AP, [1:100]). Briefly, freely floating sections were permeabilized with 0.3% Triton-X

in PBS for 2 h at room temperature, and blocked with 0.3% Triton-X in PBS containing 10% donor goat serum for one hour before incubation at 4° C with primary antibodies in blocking solution. Detection was performed using Alexa Fluor™ conjugated secondary antibodies (Invitrogen). Slices were treated for autofluorescence with 1% Sudan Black solution and cover slipped with Pro-Long™ Diamond Antifade Mountant (Invitrogen, Catalog no. P36961). Digital images were obtained using a Leica Stellaris 8 confocal microscope. Raw image z-stacks of two slices per animal were analyzed by a blinded investigator using Imaris software suite (version 9.3, Bitplane Inc., USA). The spot analysis function was utilized to generate cell counts. FIJI software [51] was used to calculate hippocampal subfield areas for density measurements.

Barnes circular maze

The apparatus used was an elevated circular platform (0.91 m in diameter) with 20 holes (5 cm diameter) around the perimeter of the platform, one of which was connected to a dark escape recessed chamber (target box) (San Diego Instruments, USA). The maze was positioned in a room with large, simple visual cues attached on the surrounding walls. The protocol used here was published elsewhere (<http://www.nature.com/protocolexchange/protocols/349>). Briefly, mice were habituated to the training room prior to each training day for 30 min in their cages. In addition, on the first day mice were placed at the center of the maze in a bottomless opaque cylinder for 60 s to familiarize the animals with the handling. Training sessions started 15 min later. Acquisition consisted of 4 trials per day for 4 days separated by a 15-min inter-trial interval. Each mouse was positioned in the center of the maze in an opaque cylinder, which was gently lifted and removed to start the session. The mice were allowed 180 s to find the target box on the first trial; all trials were 3 min long. At the end of the first 3 min, if the mouse failed to find the recessed escape box, it was gently guided to the chamber and allowed to stay in the target box for 60 s. The location of the escape box (pink circles on track plots) was kept constant with respect to the visual cues, but the location of the target hole was changed randomly. An animal was considered to find the escape chamber when its head and shoulders were above the escape box. An animal was considered to enter the escape chamber when the animal's entire body was in the escape chamber and no longer visible on the platform. Memory retention was tested 24 h after the last training session (Probe trial day 5). Briefly, the escape hole was blocked for the duration of the probe, and the time spent searching the target quadrant for the escape hole was measured for each mouse. The same parameters were

collected during acquisition and retention phases using the ANY-maze software (Stoelting Co., USA).

Spatial maze path analysis

For each day during the acquisition phase of the task, track plots were obtained for each trial after video analysis using the ANY-maze[®] software (Stoelting Co., IL, USA). Traveled paths were then classified visually using a paradigm established by prior studies [45]. Briefly, run patterns were scored as follows: 1, thigmotaxis; 2, random search; 3, scanning; 4, chaining; 5, directed search; 6, focal search; and 7, direct path. Based on this scoring scheme, 1–3 reflected non-spatial hippocampal learning, while search strategies 4–7 were considered to represent spatial hippocampal learning.

Measurements of amyloid plaques

Immunofluorescence

Immunolabeling was performed to stain amyloid plaques using 6E10 antibodies. Brain tissue was permeabilized with 0.1% Triton[™]-X100 then incubated in 10% Normal Goat serum to prevent nonspecific binding. Afterwards, the tissue was incubated with primary antibodies for 1 h using the Biowave[®] Pro system (Pelco), followed by a series of PBS washes (3×6 min), and with secondary antibodies for 1 h.

Confocal imaging

Triple-label immunofluorescence was performed as previously described in [29] using Alexa Fluor[™] – 488, – 555, – 647–conjugated secondary antibodies (Molecular Probes, Invitrogen), treated for autofluorescence with 0.1% Sudan Black solution, and coverslipped with ProLongGold mounting medium (Molecular Probes). Digital images were obtained using an Olympus IX81 FluoView1000 microscope. Raw image z-stacks were analyzed using Imaris9.3 software suite (Bitplane Scientific Software).

Western blotting

Protein concentrations were determined by using the Pierce[™] BCA protein assay.

Electrophoresis

Protein separation was done using SDS-PAGE on freshly prepared 12% SDS–polyacrylamide gels, pre-cast 10–20% SDS–polyacrylamide Tris-Tricine gels, or 10.5–14% or 4–10.5% Tris–HCl gels (Bio-Rad). Protein levels were normalized by using 2–100 µg of protein per sample (depending on the targeted protein). The samples were resuspended with 4X Tricine loading buffer and boiled for 5 min prior to loading.

Western blotting

Proteins were transferred to 0.2 µm nitrocellulose membrane (Bio-Rad) following electrophoresis. For primary neuron experiments, membranes were blocked and antibodies were diluted into Odyssey Blocking Buffer (TBS version; LI-COR Biosciences, USA). For all other experiments, membranes were blocked in TBS containing 5% bovine serum albumin (BSA; Sigma) for 1–2 h at room temperature, and probed with the appropriate antisera/antibodies diluted in 5% BSA-TTBS (TBS with 0.1% Tween-20). Primary antibodies were probed with either anti-IgG immunoglobulins conjugated with biotin, HRP or IR dyes (LI-COR Biosciences). When biotin-conjugated secondary antibodies were used, HRP- or IR-conjugated Neutravidin[®] (Pierce) or ExtrAvidin[®] (Sigma) was added to amplify the signal. Blots were revealed on a LI-COR Odyssey imaging platform (Li-Cor Biosciences).

Stripping

For re-probing, membranes were stripped using Restore[™] Plus Stripping buffer (Pierce) for 5–180 min at room temperature, depending on the antibody affinity.

Quantification

Densitometry analyses were performed using the LI-COR Odyssey software. Each protein of interest was probed in 3 individual experiments under the same conditions. Quantification by software analysis, expressed as DLUs, followed determination of experimental conditions ascertaining linearity in the detection of the signal. This method allows for a dynamic range of ~100-fold above background. Respective averages were then determined across the triplicate Western blots. Normalization was performed against actin, βIII-tubulin or NeuN, which were also measured in triplicate. The color of the signal detected at 680 nm (red by default on the Odyssey) was modified to magenta to allow colorblind individuals to distinguish both channels.

Acute slice electrophysiology

We collected acute coronal hippocampal slices (350 µm thick) from 8-month-old αSyn-KO mice. Slices were kept in ice-cold artificial CSF (ACSF) containing the following (in mM): 124 NaCl, 5 KCl, 1.25 NaH₂PO₄, 2 MgSO₄, 26 NaHCO₃, 2 CaCl₂, and 10 glucose, gassed with 95% O₂/5% CO₂, pH 7.3–7.4. Slices were incubated in ACSF at room temperature for at least 1 h before use and then transferred to an immersion recording chamber, superfused at 2 mL/min with gassed ACSF, and visualized under a Nikon Eclipse E600FN microscope (Tokyo, Japan). Picrotoxin (50 µM) and CGP54626 (1 µM) were added to the solution to block the GABA_A and GABA_B

receptors, respectively. Field excitatory postsynaptic potentials (fEPSPs) were evoked in the CA1 stratum radiatum by stimulating Schaffer collaterals (SCs) with tungsten microelectrodes (World Precision Instruments, Sarasota, FL) and recorded with ACSF-filled glass pipettes (<5 M Ω). Recordings were obtained with PC-ONE amplifiers (Dagan Instruments). Signals were filtered at 1 kHz and acquired at 10 kHz sampling rate and fed to a computer through a DigiData 1322A interface board. pCLAMP version 10.4 (Axon Instruments) software was used for stimulus generation, data display, acquisition, and storage. For baseline recording, the stimulation intensity was adjusted to obtain 40% of the maximum slope of the response and inputs were stimulated (1 ms pulse duration) every 3 s. The slope of the fEPSPs was measured between 30 and 70% of maximum. For LTP induction, a tetanic stimulation (4 trains at 100 Hz for 1 s; 30 s intervals) was applied in the SC. fEPSP slope was normalized to 10 min of baseline recording. After LTP induction, fEPSPs were recorded for 60 min. The presence of LTP was determined by comparing the last 5 min of baseline with the last 1 min of recording. Groups were compared using a one-way ANOVA. When data did not meet normality, a one-way Kruskal–Wallis test with Dunn's method post hoc was applied.

NanoString[®] nCounter[®] profiling

The nCounter[®] mouse Neuropathology panel was purchased from NanoString (NanoString Technologies, USA) and processed using the nCounter Flex analysis system (NanoString Technologies, USA). Using nSolver 4.0 software, data underwent quality control for assay efficiency, background subtraction using the mean of negative controls, and normalization using positive controls and housekeeping genes (also called CodeSet content normalization) according to manufacturer instructions. Analysis of differentially expressed genes was conducted by one or two-way ANOVA using JMP Genomics version 9.0 (SAS Institute, USA) and a false discovery rate adjusted significance threshold of 0.05. One sample was determined to be an outlier and was removed from subsequent analysis.

Pathway analysis using g:Profiler

The list of differentially regulated genes obtained through NanoString[®] nCounter[®] analysis was subjected to g:Profiler. The functional enrichment analysis was performed using g:Profiler (version e105_eg52_p16_e84549f) with g:SCS multiple testing correction method applying significance threshold of 0.05 (Raudvere, Kolberg et al., 2019). The following data sources were used: GO Molecular Function (GO:MF), GO Cellular

Component (GO:CC), GO Biological Process, KEGG, Reactome, WikiPathways, TRANSFAC, miRTarBase and CORUM.

STRING annotation & network visualization with Cytoscape

The list of differentially regulated genes obtained through NanoString[®] nCounter[®] analysis was subjected to STRING v11.5 via the stringApp v1.7.0 for Cytoscape v3.9.1 to identify and visualize possible gene clusters (Shannon et al., 2003; Szklarczyk et al., 2017). Data source settings for nodal associations were set to default with a confidence cutoff of ≥ 0.4 interaction score minimum. Gene networks were visualized using Cytoscape v3.9.1 software. Each node represents a protein, while each edge corresponds to coexpression subscores. Unless indicated otherwise, the node color reflects whether the gene is up- (orange) or downregulated (blue) while the color gradient reflects the magnitude of the change (the darker the more changed). The thickness of each edge is proportional to the STRING-based coexpression interaction between two genes (the thicker the edge, the stronger is their STRING-based association).

Statistical analyses

When variables were non-normally distributed, nonparametric statistics were used (Spearman rho correlation coefficients, Kruskal–Wallis non-parametric analysis of variance followed by Bonferroni-corrected two-group *posthoc* Mann–Whitney U tests). When variables were normally distributed, the following parametric statistics were used (one/two/three-way ANOVA or RM-ANOVA followed by Bonferroni-corrected two-group *posthoc* Student t tests or Tukey HSD test). Sample size was determined by power analysis to be able to detect statistically significant changes within a 20% variation of measured responses. Analyses were performed using JMP Pro and JMP Genomics (SAS Institute, USA). Statistical tests and outcomes are compiled in, Additional File 2: Table S2.

Results

ASO-mediated reduction of α Syn mRNA and protein in wild-type mice

For gapmer ASOs to be a viable therapeutic tool, they must selectively reduce their intended messenger RNA and be well tolerated. We tested two different ASO constructs, named ASO1 and ASO2, targeting *SNCA* transcripts using in vitro and in vivo paradigms (Additional file 1: Fig. S1). First, we exposed primary mouse cortical neurons to acute applications of these two different ASOs (300 μ g bolus) and measured the relative expression of *SNCA* mRNAs over time (Additional file 1: Fig. S1A). As expected, *SNCA* mRNA transcripts decreased over time with either ASO1 or ASO2 compared to PBS controls.

ASO2 was less effective in lowering *SNCA* mRNA abundance, with only the 48-h time point showing a decrease. By contrast, ASO1 was more effective, with a ~60% decrease in expression compared to the ~30% decrease caused by ASO2.

Since ASO1 demonstrated a strong inhibition of *SNCA* mRNA expression in cultured mouse neurons, we tested ASO1 in mice. Because we demonstrated that a 300 μg bolus of ASO1 was sufficient to lower *SNCA* transcripts *in vitro*, mice were unilaterally injected with the same 300 μg dose of ASO1 into the lateral ventricle. To document that ASO1 was equally distributed across cerebral hemispheres following ICV delivery, we performed immunohistochemical labeling and whole-section imaging (Fig. 1A). Similarly to previous reports [17], we observed that ASO1 was homogeneously localized throughout the brain 3 weeks following injection using infrared-based imaging (Fig. 1A, Additional file 1: Fig. S1B). αSyn was detected with the 4D6 antibody and used as internal control.

To assess when ASO1 was most effective in knocking down *SNCA* mRNAs, we measured *SNCA* transcriptional gene products at 2 and 3 weeks post-ASO delivery by RT-qPCR. We found that the relative abundance of *SNCA* transcripts was reduced by 34% and 48% respectively (Fig. 1B). To determine the consequence of the ASO1-induced knockdown on αSyn protein levels in targeted areas (e.g., hippocampus), confocal image analyses revealed a time-dependent reduction in αSyn and confirmed the presence of ASO1 in hippocampal cells, mirroring the observations made using infrared-based imaging (Fig. 1C). Specifically, the amount of hippocampal αSyn decreased by ~60, ~70 and ~80% at 1, 2 or 3 weeks post-ASO injection respectively (Fig. 1D). These results indicated that ASO1 suppressed αSyn mRNA and protein expression for several weeks following ICV injection.

To ensure that the ASO1 injections did not elicit an overt inflammatory reaction, we assessed the immunoreactivity profiles of ionized calcium binding

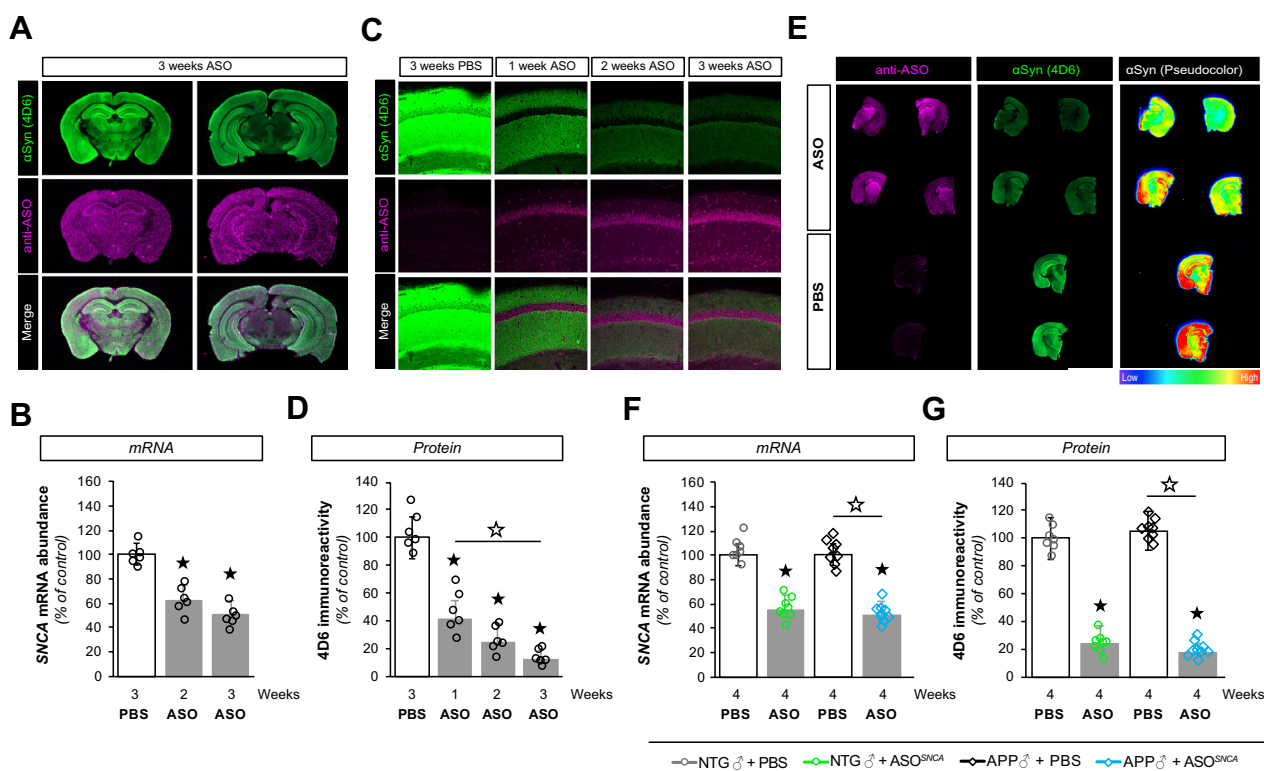


Fig. 1 ASO1 disperses throughout the brain and lowers *SNCA* gene expression. **A** Infra-red imaging documenting the widespread distribution of ASOs 3 weeks after injection using anti-ASO (pink) and anti- αSyn (4D6, green) antibodies. **B** Reduction in *SNCA* mRNA at 2 and 3 weeks post-injection as determined by RT-qPCR. **C** Confocal imaging illustrating the presence of ASO1 (pink) and a corresponding decrease in αSyn (green) in mouse hippocampi. **D** Quantification of hippocampal 4D6 immunoreactivity in ASO1 or PBS treated mice. **E** Infra-red imaging detected αSyn (green) and ASO (pink) in coronal brain sections from PBS and ASO treated mice. The relative αSyn signal was lower in ASO-injected animals than in PBS-injected animals (pseudocolor). **F, G** Measurements of *SNCA* mRNA abundance by RT-qPCR (**F**) and αSyn protein amounts by immunofluorescence (**G**) in transgenic (APP) and non-transgenic (NTG) animals treated with PBS or ASO. Histogram bars represent mean \pm SEM, $\star P < 0.05$ compared to NTG + PBS, $\star P < 0.05$ compared to APP + PBS

adaptor molecule 1 (Iba1) and glial fibrillary acidic protein (GFAP), markers of microgliosis and astrocytosis respectively in saline and ASO1-injected mice (Additional file 1: Fig. S1C). There were no differences in Iba1 or GFAP immunoreactivity between groups (Additional file 1: Fig. S1D,E).

Overall, these findings obtained in mice demonstrated that ASO1 reduced *SNCA* gene transcription in mouse neurons and brain tissues in absence of overt side effects.

Partial inhibition of α Syn expression in a mouse model of Alzheimer's disease

We previously reported that constitutive genetic deletion of *SNCA* in the J20 transgenic mouse model of AD rescues premature mortality, memory and synaptic deficits despite an exacerbation of amyloid pathology [25]. To test whether a transient lowering of α Syn could be similarly beneficial, we performed a translational study in 6-month-old non-transgenic (NTG) and J20 APP transgenic (APP) mice to assess the therapeutic potential of ASO1 on cognitive function. With this new cohort of animals, we opted to extend the intervention window to 4 weeks post-ICV delivery to minimize potential undesired effects caused by inflammatory reactions to the procedure. We first examined the distribution of ASO1 throughout the brain and measured the relative expression of *SNCA* mRNA (Fig. 1E, F). ASO1 was readily detected by antibodies raised against the chemical backbone of the ASO in animals treated with ASO1, while brain sections from PBS-injected animals showed no apparent signal (Fig. 1E, left panel). Consistent with our previous results, the new cohort of NTG animals injected with ASO1 also displayed a ~50% decrease in *SNCA* mRNA abundance (Fig. 1F). The amount of *SNCA* mRNA present in saline-treated APP transgenic animals was indistinguishable from that measured in control NTG littermates. More importantly, *SNCA* mRNA expression was reduced by half following ASO1 delivery in APP transgenic mice compared to APP animals injected with PBS. In addition, the lowering in *SNCA* transcripts was identical across ASO-treated groups, demonstrating the consistency of the knockdown induced.

We next quantified the amount of α Syn protein expression (Fig. 1E, G, Additional file 1: Fig. S2). The effect of ASO1 on α Syn brain abundance was further supported by pseudocolor images of α Syn (4D6), which readily showed higher amounts of α Syn protein in PBS-injected mice compared to ASO1-injected mice (Fig. 1E, right panel). This qualitative difference was further supported by quantitative analyses documenting that ASO1 ICV injection reduced hippocampal α Syn protein by ~80% in both APP and NTG animals (Fig. 1G). Lastly, α Syn protein abundance was measured by western blotting,

which confirmed a ~50–60% decrease in the forebrain of ASO1-injected mice compared to saline-injected animals (Additional file 1: Fig. S2). These findings indicate that α Syn-targeting ASOs consistently and robustly lower *SNCA* mRNA and α Syn protein in vivo.

Lowering α Syn rescues cognitive deficits in male APP mice

We previously demonstrated that ablating the *SNCA* gene in APP mice improved cognition using a genetic approach [25], suggesting that reducing α Syn expression might constitute a putative translational strategy to alleviate memory deficits. To examine this possibility, both APP and NTG mice were subjected to the Barnes circular maze (BCM), a hippocampal-dependent spatial reference memory task, four weeks post-injection. In contrast to our earlier genetic study which only used male mice [25], and given the importance of sex as a biological variable for biomedical research, here we evaluated both male (Fig. 2) and female animals (Fig. 3).

During the acquisition phase of the task, the male PBS-injected NTG and APP mice (NTG + PBS and APP + PBS respectively) were able to learn the task as assessed by decreased latencies. However, APP animals displayed a mild acquisition deficit (Fig. 2A), consistent with previous reports [25, 30]. APP mice that received a single bolus of ASO1 (APP + ASO^{*SNCA*}) displayed decreased latency compared to saline-injected APP littermates. There was no difference in the latencies of the ASO-injected APP and NTG mice on day 5 (Fig. 2A). Paralleling these observations, similar changes were also observed for the distance traveled by the animals during the task (Fig. 2B), suggestive of better spatial memory function.

However, APP mice are well-known to be hyperactive [25, 62] and we previously documented that *SNCA* deletion can alleviate this hyperactivity phenotype [25]. As expected, saline-injected APP mice traveled the most during the 5-day acquisition stage. Importantly, the ASO-injected APP mice traveled shorter distances to the escape hole than the PSB-injected APP mice (Fig. 2B). There was no difference in distance traveled between the ASO-injected APP and the NTG mice on any acquisition learning day (Fig. 2B), likely the result of an amelioration of hyperactive behavior.

Genetic deletion of *SNCA* also normalized the characteristic freezing behavior of APP mice to baseline levels of NTG littermates [25]. Consistent with our previous study, APP + PBS mice froze more than NTG + PBS or NTG + ASO^{*SNCA*} groups (Fig. 2C). The APP + PBS mice also froze more than ASO-injected APP mice, whose behavior was indistinguishable from the NTG groups. This alleviated freezing behavior in APP + ASO^{*SNCA*} animals indicated that a reduction in *SNCA* transcriptional

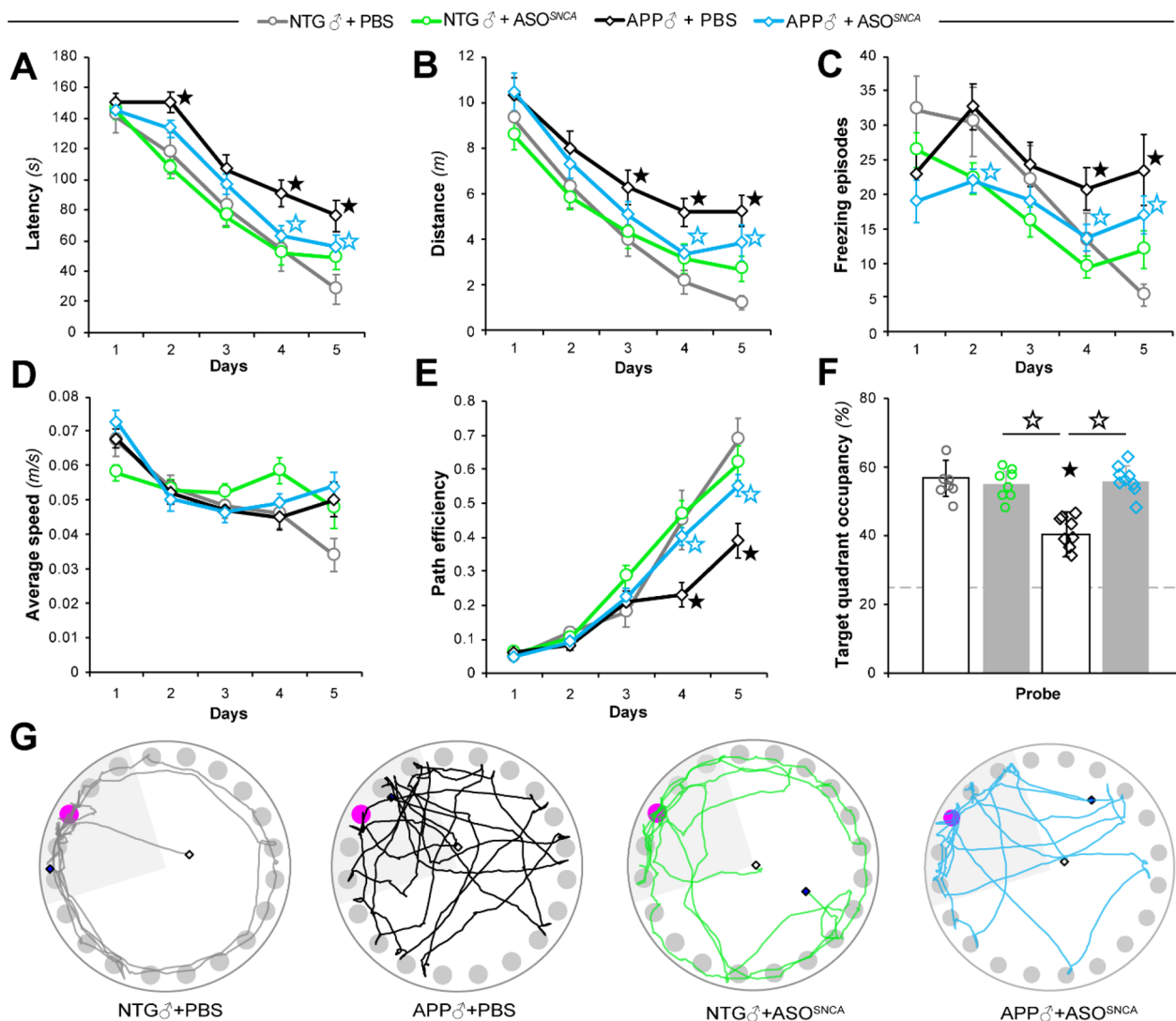


Fig. 2 Behavioral effects of α Syn reduction in male NTG and APP mice. Male APP and NTG controls were tested in the Barnes circular maze (BCM) at six months of age. **A, B** Spatial learning of the BCM task was reflected by reductions in escape latency (**A**) and distance traveled (**B**). **C, D** Measurements of freezing episode numbers (**C**) and average animal speed (**D**) in the BCM task were used to assess phenotypic changes other than spatial learning. **E** Quantitative assessment of animal trajectories during the learning phase using path efficiency. **F, G** Spatial memory retention in the BCM task was determined by target quadrant occupancy (**F**) and by assessment of path traces (**G**). Data represent mean \pm SEM; $\star P < 0.05$ compared to NTG + PBS, $\star P < 0.05$ compared to mice of the same genotype in the other treatment group, $n = 8$ mice/treatment/genotype

products can return APP mice to a normal behavioral phenotype.

Of note, there were no differences in average speed between any of the groups (Fig. 2D). These findings likely indicated that the decrease observed in distance traveled was not simply due to a global reduction in locomotor behavior in APP mice but perhaps corresponded to more efficient trajectories during the learning phase.

To directly address this possibility, path length efficiency, defined as the path taken by the mouse compared to the shortest possible route to the escape hole, was

measured. By the end of the acquisition phase, all groups but the APP + PBS mice displayed robust increases in path efficiency (Fig. 2E). Importantly, the ASO-injected APP mice were more efficient than the PBS-injected APP mice on days 4 and 5. Altogether, measures of latency, distance traveled and path length efficiency were consistent with better spatial learning memory in APP + ASO^{SNCA} mice compared to PBS-treated APP animals.

On the final day of the BCM task, a probe trial was conducted to evaluate memory retention in all tested groups. As expected, the target quadrant occupancy

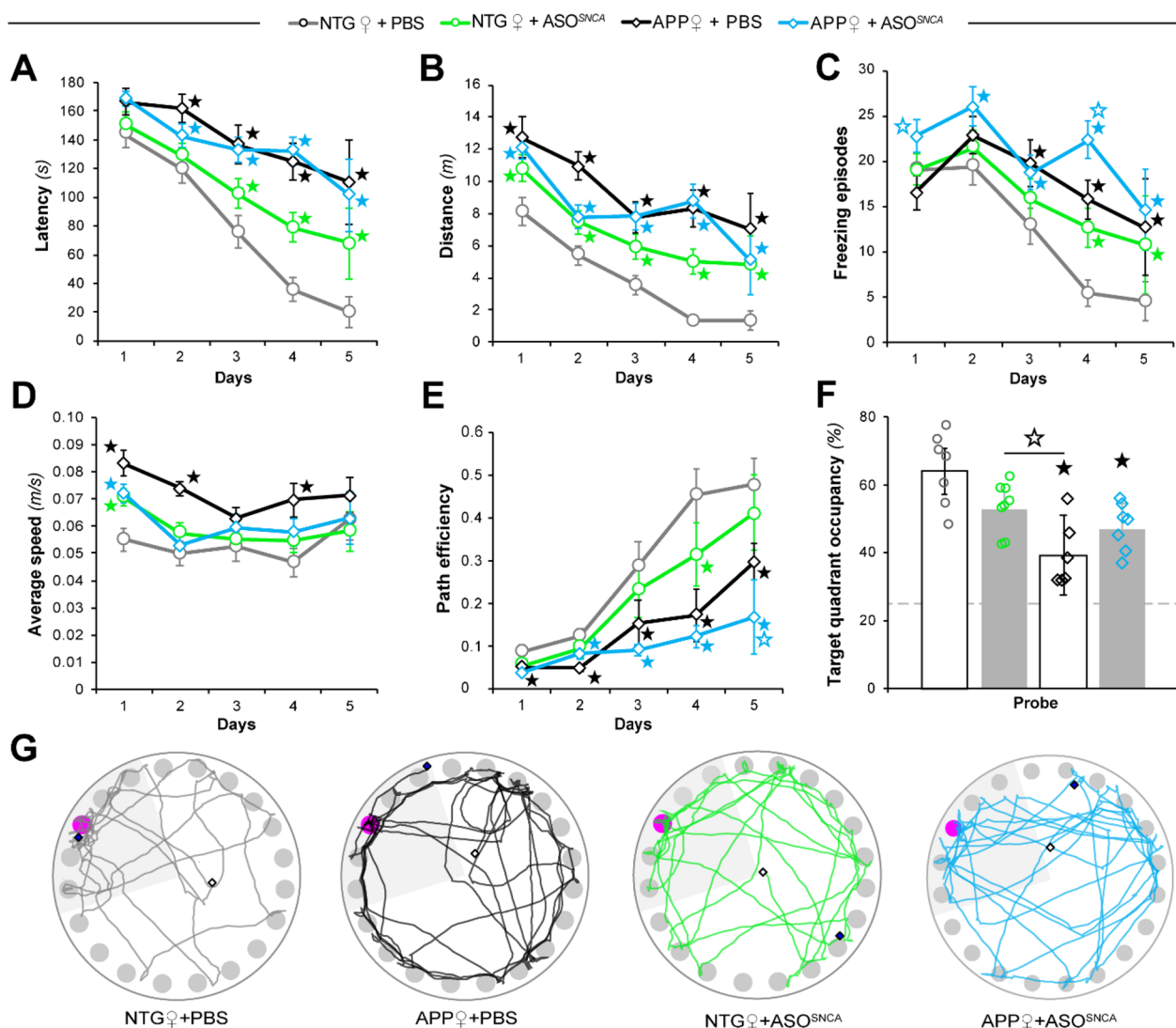


Fig. 3 Behavioral effects of α Syn reduction in female NTG and APP mice. Female APP and NTG controls were tested in the Barnes circular maze (BCM) at six months of age. **A, B** Spatial learning of the BCM task was reflected by reductions in escape latency (**A**) and distance traveled (**B**). **C, D** Measurements of freezing episode numbers (**C**) and average animal speed (**D**) in the BCM task were used to assess phenotypic changes other than spatial learning. **E** Quantitative assessment of trajectories used by animals during the learning phase using path efficiency. **F, G** Spatial memory retention in the BCM task was determined by target quadrant occupancy (**F**) and by assessment of path traces (**G**). Data represent mean \pm SEM; $\star P < 0.05$ compared to NTG + PBS, $\star\star P < 0.05$ compared to mice of the same genotype in the other treatment group, $n = 8$ mice/treatment/genotype

for the NTG + PBS group was higher than that of the APP + PBS group (Fig. 2F). Injecting *SNCA*-targeting ASO1 in NTG mice did not alter retention compared to NTG + PBS animals. However, the APP + ASO^{SNCA} group performed significantly better than the APP + PBS group and similarly to both NTG groups (Fig. 2F). This apparent rescue in spatial memory retention was also reflected in the track plots from each group (Fig. 2G). These results indicate that both acquisition and retention of spatial reference memory was

improved in male APP mice just four weeks after a single injection of ASO^{SNCA}.

Reducing α Syn selectively worsens cognition in female mice

In an effort to rigorously consider biological variables essential to neurological diseases, female APP mice were subjected to the same behavioral testing as the male mice (Fig. 3). As expected, NTG saline-injected female mice had shorter latencies to the escape hole than APP + PBS

female mice (Fig. 3A). Unlike male animals, however, it was surprising that NTG+ASO^{SNCA} female mice had longer latencies than NTG+PBS mice on days 3–5. Importantly, APP mice that received ASO^{SNCA} displayed similar latencies to the APP+PBS female control mice, indicating that there was no effect of ASO administration on the female APP mice (Fig. 3A). This pattern repeated itself in the analysis of distance traveled, whereby ASO^{SNCA} injection increased the distances traveled by NTG females and failed to alter the distance traveled by APP mice (Fig. 3B).

Because both latency and distance traveled in the BCM task can be impacted by alterations in freezing behavior and animal speed, we analyzed both of those variables for each group of female mice. Although the number of freezing episodes decreased over training in NTG+PBS female mice, their number remained elevated in the NTG+ASO^{SNCA} group (Fig. 3C). Here again, ASO^{SNCA} injection did not decrease freezing behavior in APP mice, and in fact exacerbated it on days 1 and 4 (Fig. 3C). Next, we examined the average speed of the animals, an important variable when considering locomotor hyperactivity previously described in male J20 mice [62]. Apart from the first day, there was no difference in speed between the NTG+PBS females and the NTG+ASO^{SNCA} females (Fig. 3D). Unexpectedly, the APP+PBS females had higher average speeds than the NTG+PBS females on days 1, 2 and 4. By contrast, the average speeds displayed by APP+ASO^{SNCA} mice were similar to those of the NTG groups (Fig. 3D). However, unlike in males, reducing *SNCA* mRNA and protein did not rescue the hyperactivity and freezing phenotypes observed in APP animals, suggesting sex differences in α Syn expression or function.

As additional evidence of spatial learning, we evaluated path length efficiency. NTG females, whether injected with PBS or ASO, improved their path efficiency over time (Fig. 3E). APP+PBS females also improved their path efficiency, though not as much as NTG+PBS animals. The APP+ASO^{SNCA} females used less efficient paths to reach the escape target than the NTG+PBS and were largely like the APP+PBS female groups (Fig. 3E). Contrary to the effect we observed in male animals, administering ASO^{SNCA} worsened the spatial learning of female mice irrespective of transgene expression.

Next, we determined spatial reference memory retention by subjecting animals to a probe trial on the last day of the task (Fig. 3F). Even though target quadrant occupancy trended towards a decrease in NTG+ASO^{SNCA} animals compared to NTG+PBS mice, both groups were statistically similar. As expected, the APP+PBS females spent less time in the correct quadrant than both the NTG+PBS and the NTG+ASO^{SNCA} females (Fig. 3F).

The NTG+ASO^{SNCA} females performed better than the APP+PBS group. Consistent with persisting learning deficits, ASO^{SNCA} injection did not improve the probe trial performance of the APP females, who performed no differently than the APP+PBS mice. The representative track plots from each group further supported the quantitative analysis of the probe trial and illustrated the lack of rescue in APP mice (Fig. 3G).

Despite well-established sex differences across multiple APP transgenic models whereby earlier-onset amyloid pathology has been consistently noted in females [22], gender effects on A β pathology have not been systematically reported for the J20 APP mouse model. For these reasons, and because transiently lowering α Syn could affect amyloid burden, we aimed to determine whether ASO^{SNCA} delivery altered A β deposition in J20 mice in a sex-specific manner. To this end, we measured amyloid burden using confocal imaging analysis (Additional file 1: Fig. S3A) as previously reported [25]. Quantitative analyses of hippocampal A β deposits revealed no differences in amyloid loads between sexes in 6-month-old APP+PBS or APP+ASO groups (Supplementary Fig. 3B, Additional file 1), arguing against a potential impact of A β pathology on the observed behavioral phenotype.

Altogether, these data revealed an unexpected sex difference in the response to α Syn-lowering ASOs in APP transgenic mice. Importantly, these findings also demonstrated gender-specific responses to mouse ASO^{SNCA} in NTG mice, whereby knock-down of *SNCA* transcripts resulted in learning and retention deficits of spatial memory in female mice compared to male mice.

Differential role of α Syn on cognition in male and female mice

Since the sex-specific behavioral effects observed as a result of the *SNCA* knockdown implied that α Syn might function differently in male and female brains, we investigated whether the genetic deletion of *SNCA* would differentially impact learning and memory in male and female animals. In line with previously published results from our group [25], α Syn-KO males performed no differently than age-matched non-littermate NTG mice based on latency (Fig. 4A) and distance (Fig. 4B) measurements. Female NTG mice were indistinguishable from the NTG and α Syn-KO males on both latency and distance parameters. To our surprise, and in sharp contrast with male animals, α Syn-KO female mice displayed clear deficits. They displayed longer latencies and traveled longer distances to reach the escape hole compared to both NTG females and α Syn-KO males, indicating that ablating α Syn was detrimental to the spatial learning of female mice (Fig. 4A, B; respectively).

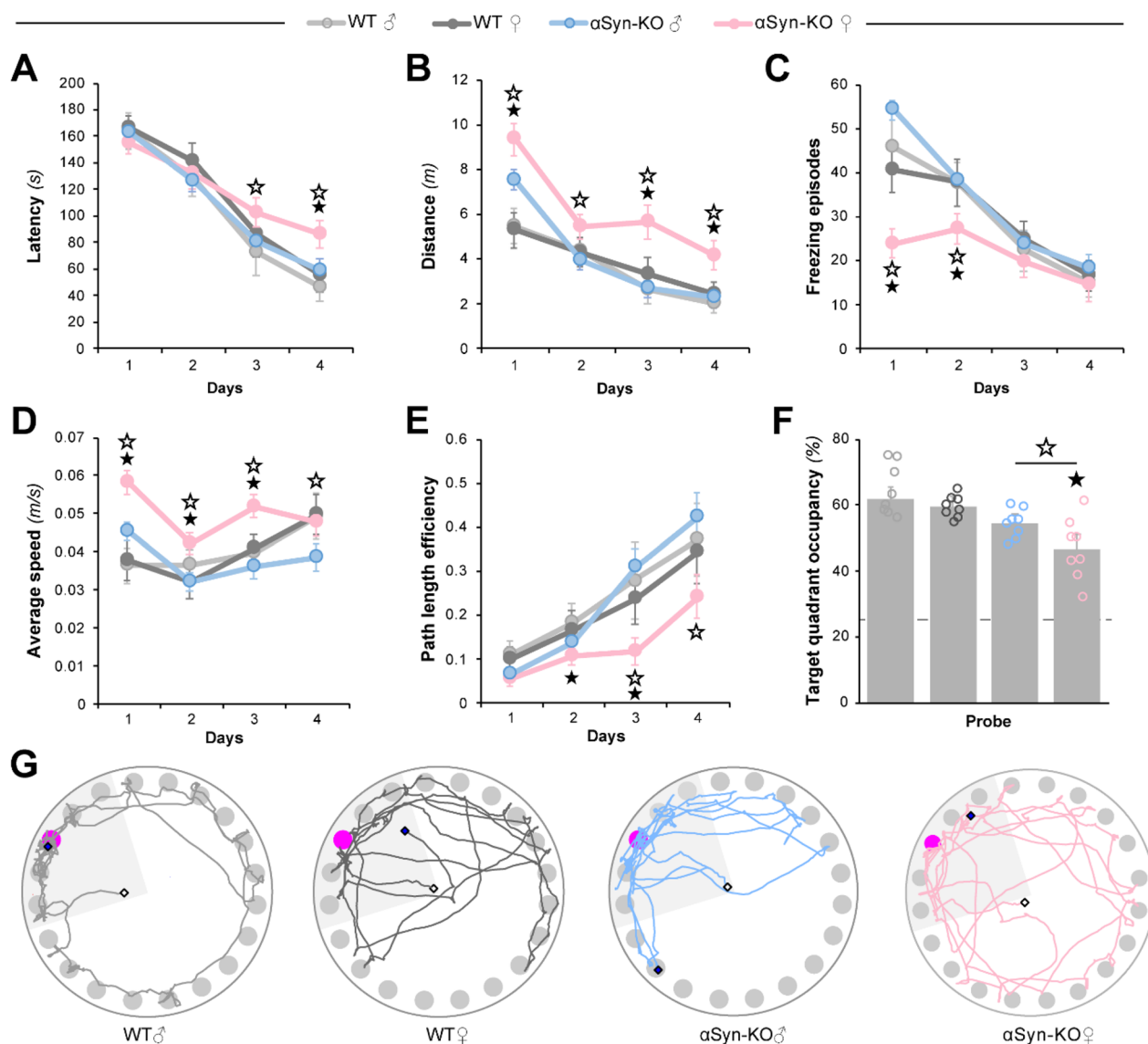


Fig. 4 Genetic ablation of α Syn negatively impacts the performance of female mice on the Barnes circular maze. Male and female α Syn knock-out mice (α Syn-KO) and wild-type C57BL/6 J controls were tested in the Barnes circular maze (BCM) at six months of age. **A, B** Spatial learning of the BCM task was reflected by reductions in escape latency (**A**) and distance traveled (**B**). **C, D** Measurements of freezing episode numbers (**C**) and average animal speed (**D**) in the BCM task were used to assess phenotypic changes other than spatial learning. **E** Quantitative assessment of trajectories used by animals during the learning phase using path efficiency. **(F-G)** Spatial memory retention in the BCM task was determined by target quadrant occupancy (**F**) and by assessment of path traces (**G**). Data represent mean \pm SEM; $\star P < 0.05$ compared to WT mice of the same sex, $\star P < 0.05$ compared to mice of the same genotype and opposite sex, $n = 8$ mice/genotype/sex

To gain a more complete picture of other putative changes in α Syn-KO female mice, we also measured freezing and average speed to better characterize baseline locomotor activity in each group. Male and female NTG mice displayed equivalent freezing episodes (Fig. 4C) and had comparable average speeds (Fig. 4D). α Syn-KO males froze the same amount as NTG mice. At the beginning of the acquisition phase of the task, α Syn-KO females froze less often than both α Syn-KO male littermates and

female NTG mice, though this behavior faded over time (Fig. 4C). The average speed of male and female NTG mice was equivalent, and α Syn-KO males were no different than the NTG groups. However, female α Syn-KO mice elicited greater average speeds than NTG females and male α Syn-KO littermates on days 1, 2 and 3. This difference also persisted on day 4 when compared to α Syn-KO males, though at that point of learning female α Syn-KO mice were no longer different from NTG

animals (Fig. 4D). The combined observation that female α Syn-KO mice traveled larger distances, moved faster and with fewer freezing episodes during the first two days of training, was suggestive of a hyperactive phenotype early in the task.

Because this hyperactivity could also affect path length efficiency, we examined whether gender differences impacted spatial navigation. Male and female NTG mice took paths of equivalent efficiency to the escape hole, and α Syn-KO males were similarly efficient (Fig. 4E). Though all groups improved their path efficiency over time, female α Syn-KO mice were the least efficient and their spatial navigation was worse than that used by male α Syn-KO littermates on acquisition days 3 and 4 (Fig. 4E). To determine whether male and female α Syn-KO mice used similar learning strategies, track plot videos were analyzed as previously described [18, 45]. The relative distribution of different search strategies used by male and female α Syn-KO mice revealed that both groups relied on similar spatial learning strategies (Supplementary Fig. 4A, B, Additional file 1), possibly indicating a differential encoding of memory traces across sexes in α Syn-KO animals.

On the last day of testing, a probe trial was conducted to assess spatial memory retention. The NTG mice all demonstrated strong spatial memory retention, as they spent ~60% of their time in the target quadrant during that retention test (Fig. 4F). Male α Syn-KO mice spent the same amount of time in the target quadrant as the NTG mice. Female knockout mice, however, spent less time in the target quadrant than both female NTG mice

and male α Syn-KO mice (Fig. 4F). The difference in target quadrant occupancy was also evident when comparing representative traces from each group (Fig. 4G).

Considering that potential sex-dependent differences in α Syn brain expression could exist, we measured the relative α Syn protein abundance in the hippocampi of WT mice while α Syn-KO mice served as internal negative controls (Supplementary Fig. 5, Additional file 1). No differences in hippocampal α Syn protein abundance were detected across sex. Because synuclein family members could compensate for the absence of α Syn, we also measured β -synuclein and found no differences across groups.

We next considered the possibility that female α Syn-KO mice could display an earlier onset of putative spatial memory deficits than α Syn-KO males. To directly test this hypothesis, we compared spatial learning and retention of young (6-month-old) and middle-aged (12-month-old) male α Syn-KO mice in the BCM task (Supplementary Fig. 6, Additional file 1). With the exception of a slight difference in average speed across age groups, all other variables examined (i.e. latency, distance traveled, freezing episodes and path efficiency) were indistinguishable (Additional file 1: Fig. S6A–E). Spatial memory retention was similar between young and middle-aged α Syn-KO males (Additional file 1: Fig. S6F), a conclusion further supported by corresponding track plots (Additional file 1: Fig. S6G).

With these potential interpretations excluded, these findings revealed that the function of α Syn in learning and memory differs between male and female brains.

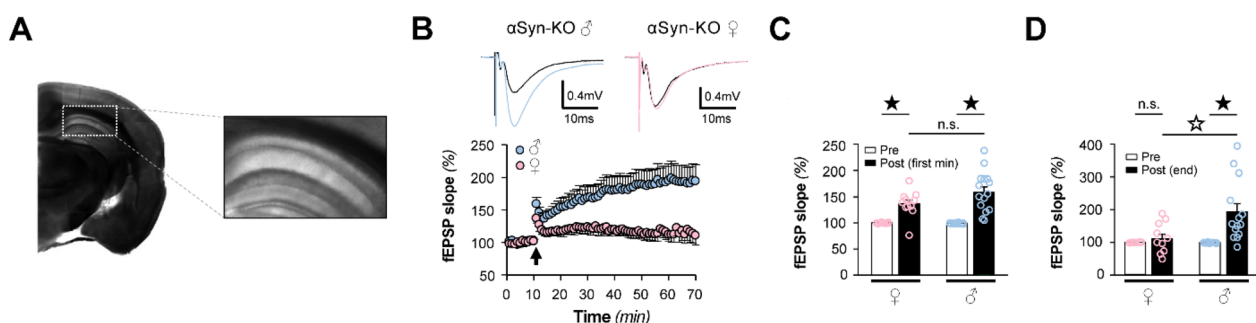


Fig. 5 Sex differences in α Syn-KO mice hippocampal LTP. **A** Field excitatory postsynaptic potentials (fEPSPs) were recorded at CA1 synapses by stimulating the Schaffer collaterals. **B** *Top*, Representative fEPSP traces before (black) and after a high-frequency stimulation (HFS) of the Schaffer collaterals recorded from male (blue) and female (pink) α Syn-KO mice. *Bottom*, fEPSPs recorded from hippocampal CA1 during long-term potentiation induced by HFS of Schaffer collaterals (100 Hz, 1 s) of α Syn-KO females ($n = 12$, pink) and males ($n = 14$, blue). Arrowhead indicates application of HFS. **C**, **D** fEPSP slopes 1 min (**C**) and 60 min (**D**) following HFS (post), relative to baseline established prior to HFS (pre), from female and male α Syn-KO mice. Data are expressed as mean \pm SEM; $\star P < 0.05$ compared to pre-HFS within the same sex group, $\star P < 0.05$ compared to mice to opposite sex

Differential role of α Syn on long-term potentiation in male and female mice

We next determined whether long-term potentiation (LTP), a cellular mechanism widely assumed to underlie learning and memory, was altered in α Syn-KO mice based on sex. We induced LTP in acute hippocampal slices from 8-month-old α Syn-KO female and male mice (Fig. 5A). High-frequency stimulation (HFS) of the Schaffer collaterals elicited normal initial potentiation in both sexes (Fig. 5B, C). One minute following induction, the percent potentiation was $36.8 \pm 6.9\%$ in females and $58.8 \pm 10.4\%$ in male slices. However, this initial potentiation failed to stabilize in female slices, with responses decaying to control levels over the hour post HFS, while potentiation in male slices was stable and robust (Fig. 5B, D). Sixty minutes following HFS, the percent potentiation was $10.56 \pm 14.6\%$ in females and $94.14 \pm 24.8\%$ in males.

Together, these electrophysiological results demonstrate that LTP is impaired in female α Syn-KO hippocampal slices compared to male animals.

Identification of a differentially expressed gene network centered around *EGR1* in the hippocampi of *SNCA*-null mice

To determine the underlying molecular mechanism supporting this sex-dependent role of α Syn on spatial learning and synaptic plasticity, we performed a NanoString[®] transcriptional profiling of hippocampal tissues from wild-type (WT) and α Syn-KO mice based on sex. Unsupervised hierarchical clustering of the normalized dataset readily segregated hippocampal datasets by genotype, while sex representation was slightly more heterogeneous (Additional file 1: Fig. S7A). Principal component (PC) analysis revealed

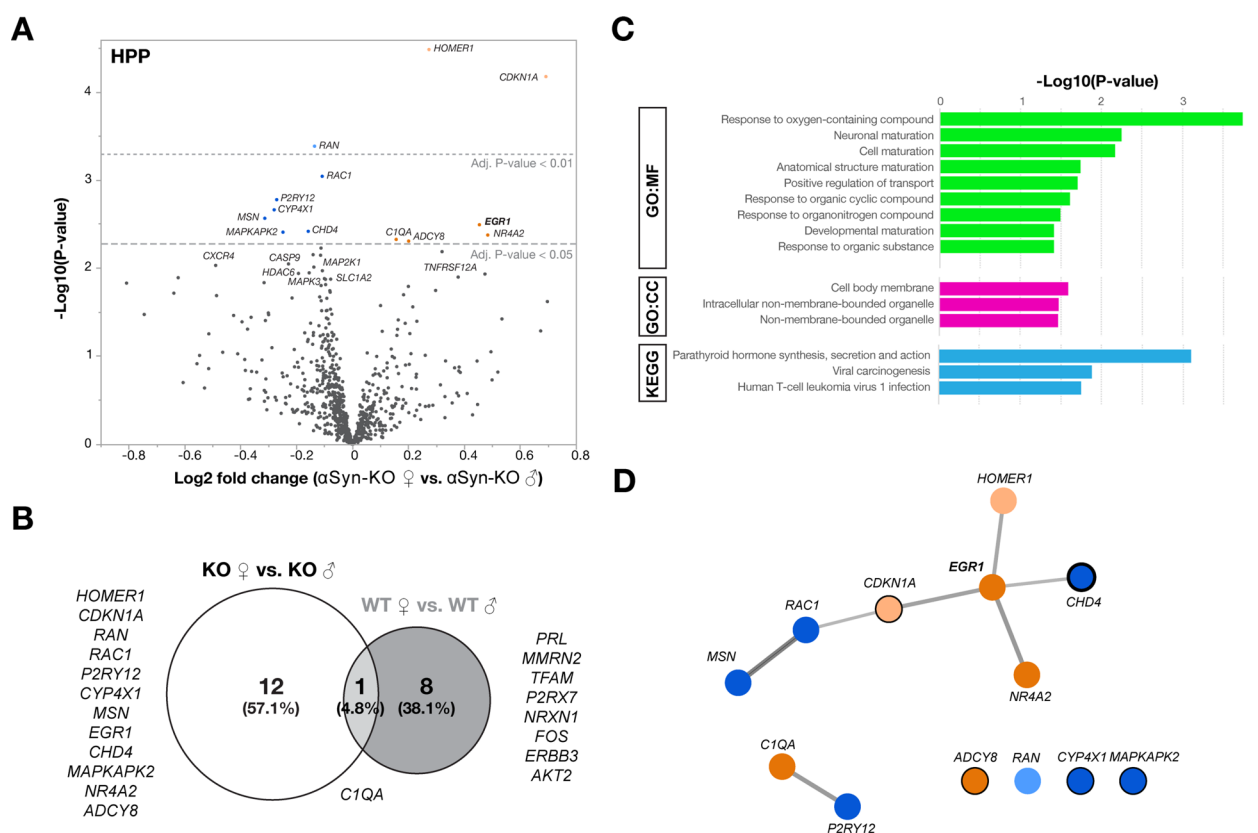


Fig. 6 Differential gene expression in male and female α Syn-KO mice. NanoString[®] transcriptional profiling was performed on hippocampal RNA from 6-month-old female and male α Syn-KO mice. **A** Volcano plot of the differentially expressed genes of α Syn-KO females compared to α Syn-KO males at adjusted significance thresholds of $P < 0.05$ and $P < 0.01$. Orange indicates upregulated genes, blue indicates downregulated genes. **B** Venn diagram of differentially expressed genes shows little overlap between WT and α Syn-KO females and males. **C** Top results for GO and KEGG databases using the female and male α Syn-KO differentially expressed gene list performed with g:Profiler for functional enrichment analysis. **D** MCL clustering and visualization of Cytoscape clusters was performed using clusterMaker2 based on co-expression data. Analysis revealed *EGR1* as a central node in the network as well as several *EGR1* target genes (black circles, *thickness* reflects the number of responsive elements)

a dominant effect of PC1 (39%), resulting in the clustering of the animals based on genotype, whereas other PCs accounted for less than 8% (Additional file 1: Fig. S7B). Comparing female and male α Syn-KO mice, 13 genes were differentially expressed including *HOMER1A*, *CDK1NA*, *RAN*, *RAC1*, *P2RY12*, *CYP4X1*, *MSN*, *EGR1*, *CHD4*, *MAPKAPK2*, *NR4A2*, *CIQA* and *ADCY8* (Fig. 6A, B). Only one of these genes, *CIQA*, was also common with differentially expressed genes when comparing female and male hippocampi in WT mice (Fig. 6B). Pathway analysis identified response to oxygen-containing compound, neuronal maturation

and cell maturation (Fig. 6C). Importantly, network analyses using Cytoscape [55] identified a differentially expressed gene network centered around *EGR1*, a central modulator of learning and memory [24, 60], in the hippocampi of α Syn-KO mice (Fig. 6D). Of note, 5 out of the 12 gene hits (*CDK1NA*, *CHD4*, *CYP4X1*, *MAPKAPK2* and *ADCY8*) correspond to gene targets of the transcription factor Egr1, also known as Zif268 (Fig. 6D, black circles).

To validate this finding, we performed confocal image analyses following immunofluorescent labeling of Egr1 in male and female α Syn-KO mice (Fig. 7A). As

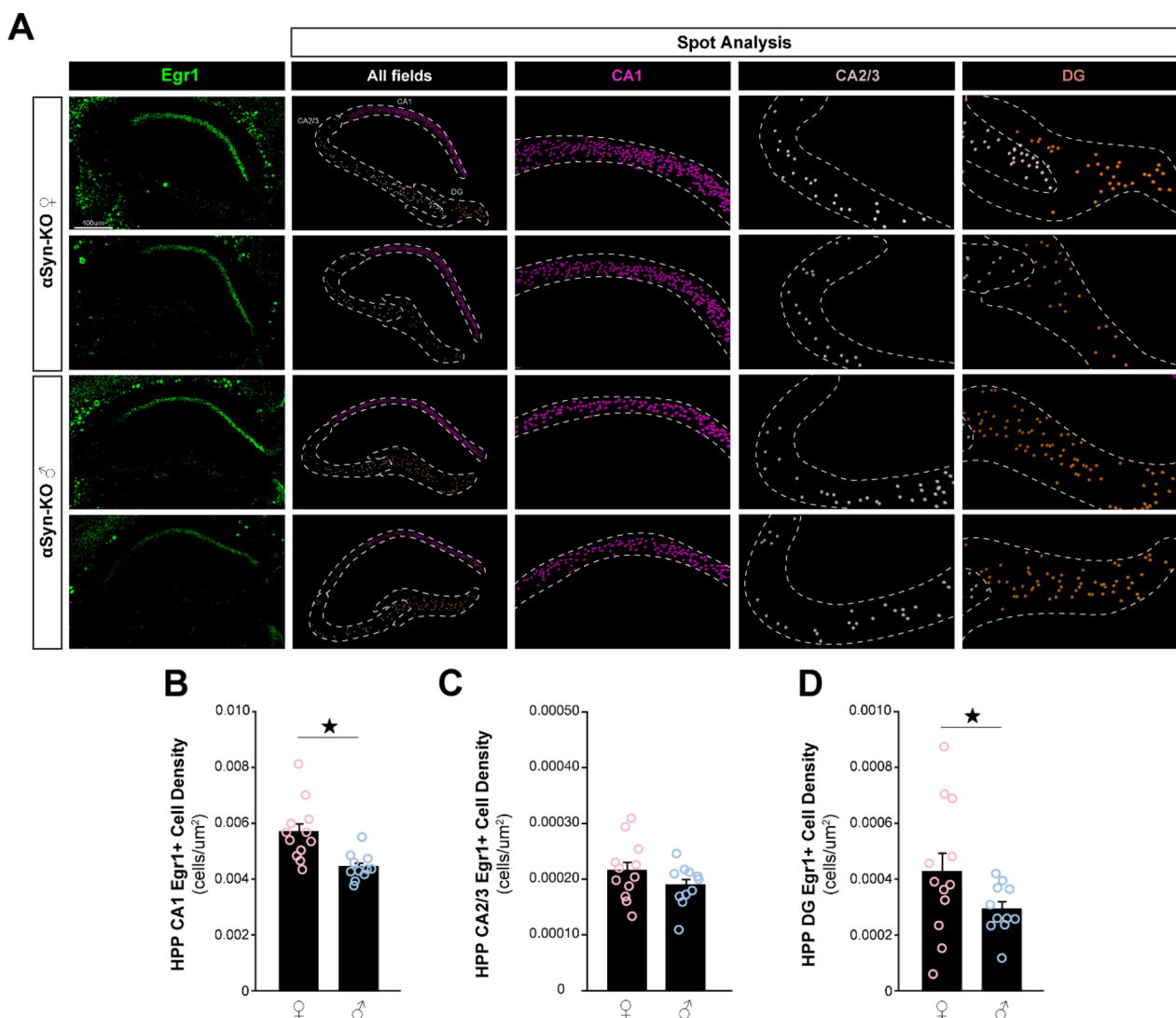


Fig. 7 Egr1 protein expression in the hippocampus of α Syn-KO mice. Immunofluorescence labeling and confocal microscopy image analysis of hippocampal slices from male and female α Syn-KO mice were performed for Egr1 density. **A** Representative 20 \times confocal images for Egr1 (green) and corresponding segmentations using Imaris spot analysis (CA1, magenta; CA2/3, grey; DG, brown). Hippocampal regions are indicated by dashed white lines while Egr1-positive neurons are indicated by spots. **C, D** Cell density analysis of Egr1-expressing neurons in CA1 (**B**), CA2/3 (**C**) and dentate gyrus (DG; **D**). Histogram bars represent mean \pm SEM, $\star P < 0.05$, $n = 6$ mice/sex, 2 slices/mouse

previously documented [43], *Egr1* was preferentially expressed in CA1 excitatory neurons and more sparsely in other hippocampal fields, i.e. CA2, CA3 and dentate gyrus (DG). Using Imaris spot analysis, we found that *Egr1*-positive density was elevated in female mice compared to male littermates in the CA1 and DG (Fig. 7B, D). By contrast, no difference was observed in the CA2/3 region (Fig. 7C).

Overall, these results thus revealed a novel connection between α Syn and *Egr1* in a sex-specific manner (Supplementary Fig. 8, Additional file 1).

Discussion

Accumulating evidence from our group and others has implicated α Syn as a potentiator of AD [3, 13, 25, 29, 30, 56]. Based on the demonstration that *SNCA* ablation rescued cognitive deficits in male APP mice [25], we hypothesized that transient lowering of α Syn expression through the use of an ASO targeting *SNCA* mRNA would alleviate memory deficits in the same APP mouse model. We found that a single injection of a murine ASO^{*SNCA*} was effective at decreasing *SNCA* mRNA and protein abundance in mice. As predicted by our hypothesis, ASO^{*SNCA*} administration improved spatial reference memory in APP mice. Surprisingly, we observed this therapeutic benefit in male, but not female, animals. Furthermore, behavioral experiments using constitutive α Syn-KO mice revealed a sex-specific role of α Syn for spatial learning and memory. To gain functional insights into these differences across sexes, we performed electrophysiological recordings and transcriptional profiling. These experiments revealed previously unknown differences in hippocampal LTP between males and females, and in α Syn-dependent gene expression patterns, including a network of differentially regulated genes centered around *EGRI*, a critical modulator of long-term learning and memory. Overall, these results have two important consequences: 1) they provide a novel proof-of-principle demonstration that reducing α Syn expression in AD is a likely viable translational strategy only in male subjects, and 2) they document a novel function of α Syn on long-term spatial memory which differs between male and female brains.

ASO-mediated knockdown of α Syn rescues memory deficits in male APP mice

ASOs have been increasingly used in recent years to modify protein expression in neurological disorders [5, 47]. Earlier studies in mouse models of spinal muscular atrophy (SMA) demonstrated that delivery of ASOs into the lateral ventricle were effective at modifying target mRNA splicing and functional protein abundance in brain tissue [41]. Human clinical trials yielded transformative results,

with improved motor function and survival in children diagnosed with SMA who received the Nusinersen ASO (Spinraza®), which led to its rapid approval by the FDA [36]. The recent successes of ASO therapies in SMA and Duchenne muscular dystrophy [28] has sparked interest in applying similar strategies to other degenerative diseases [14, 47]. While synuclein proteins are common targets of clinical trials for PD, Lewy Body Dementia and Multiple System Atrophy, few trials are currently targeting synuclein proteins to screen patients or to improve outcomes in AD (<https://clinicaltrials.gov/>).

Prior work from our group demonstrated that constitutive *SNCA* ablation in male J20 APP transgenic mice, a commonly used model of AD, alleviated memory deficits [25]. In this study, we used a murine ASO^{*SNCA*} to demonstrate that transient knockdown of α Syn could rescue cognition. We showed that the resulting lowering of α Syn rescued cognitive deficits in male APP mice, consistent with our previous results [25]. Thus, the combined results from ASO^{*SNCA*}-injected APP mice and from APP/ α Syn-KO mice indicate to us that ASO^{*SNCA*} might be a viable treatment option for men with AD-associated cognitive deficits.

We readily acknowledge that the results presented here relied on the use of transgenic APP mice. We previously reported that our J20 mice overexpress approximately threefold more APP than NTG mice [25, 29, 30, 39], a finding recently validated [23]. Consequently, we cannot rule out the possibility that the memory impairments seen in J20 mice are due to human APP overexpression. However, newer studies have demonstrated that behavioral and neural network abnormalities in J20 APP transgenic mice resemble those of *APP* knock-in mice [23], thus indicating that familial AD-linked *APP* mutations cause spatial learning and memory deficits in absence of *APP* overexpression. This said, future studies using *APP* knock-in animals [50] will be needed to address whether the gene deletion of *SNCA* or ASO^{*SNCA*} treatment can also rescue memory deficits in these models.

Differential role of α Syn in learning and memory based on sex

The cognitive rescue caused by the murine ASO^{*SNCA*} treatment was only seen in male APP animals. Surprisingly, NTG female mice performed worse on spatial reference memory tasks when injected with ASO^{*SNCA*}, while treated female APP mice showed no cognitive amelioration. To further demonstrate a differential role of α Syn across sexes in spatial learning and memory, we next determined whether female mice would be impaired if *SNCA* was constitutively ablated. As reported previously [9, 25], α Syn-KO males performed no differently than age-matched non-littermate NTG mice on

hippocampal-dependent spatial reference memory tasks. Female α Syn-KO mice, however, displayed learning and retention memory impairments compared to both α Syn-KO males and NTG females. To our knowledge, these findings are the first to document a sex effect in response to *SNCA* knockdown or ablation, demonstrating that α Syn function differs in male and female brains.

Abeliovich et al. [1] originally described *SNCA*-KO male and female mice on a mixed 129/SvJxC57BL/6 genetic background. They found no differences between male and female mice on the open-field locomotor testing paradigm, but did not assess spatial memory. In addition, these same authors reported no differences in CA1 LTP between *SNCA*-KO and wild-type slices. However, the sex of the animals used in those electrophysiology experiments was not documented, making comparison to our data impossible. Another group reported no differences in hippocampal synaptic plasticity in α Syn and β -synuclein (β Syn) single KO mice as well as α Syn/ β Syn double KO animals [10]. Their results using exclusively male mice are consistent with the lack of LTP and spatial learning deficits observed in our current and past studies. It is possible that the effects of sex documented here were masked in other work by the absence of dedicated groups to study sex as a key biological variable, as recently highlighted [37].

Despite the recurring evidence that sex can impact disease pathogenesis [31, 59], prior studies utilizing ASOs targeting *SNCA* often used mice of a single sex, when sex is reported at all, or did not examine data for possible sex effects [2, 7, 12, 42, 58, 63]. Lack of analysis and reporting could obscure important differences and delay the development of clinical therapies [37]. To our knowledge, our report is the first observation demonstrating that genetic ablation of *SNCA* differentially affects the cognition of male and female mice. Thus, reports of the beneficial effects of α Syn reduction based on experiments using exclusively male animals should not be assumed to apply similarly to females.

EGR1 as a key mediator of spatial memory

There is overwhelming evidence demonstrating that *EGR1*-mediated transcriptional mechanisms play critical roles in neuronal plasticity, memory formation and consolidation (see for review [61]). These functions appear to fundamentally depend on multiple factors including: 1) a complex relationship between *EGR1* expression dosage, 2) the temporal expression of *EGR1* (e.g. acute vs. sustained expression) [21], 3) the type of memory process involved [53], and 4) the underlying brain regions [6, 24, 43, 61]. For these reasons, it has been proposed that *EGR1* can induce beneficial or deleterious effects [64]

and that the outcome may depend on the target genes downstream of *EGR1* [61]. There is also existing evidence that *EGR1* can have sex-specific effects on behavior [15, 57] and that mouse strain can influence the expression of *EGR1* [44].

Several studies have documented an upregulation of *EGR1* at transcriptional and post-translational levels in AD brain tissue and in mouse models of the disease [4, 19, 20, 26, 33, 34]. Briefly, microarray analyses revealed that hippocampal *EGR1* transcriptional expression increased with AD severity [20]. Subsequent studies reported Egr1 protein elevations in cognitively-impaired Tg2576, APP/PS1 and 3xTg-AD mouse models of AD [4, 19, 26]. Conversely, knockdown of *EGR1* improved cognitive deficits in 3xTgAD mice [46]. Overall, these studies suggest that sustained elevated expression of *EGR1* is detrimental for long-term memory.

In our own studies, transcriptional profiling analyses revealed an increase in *EGR1* transcripts in the hippocampi of female α Syn-KO mice compared to male littermates. We confirmed the elevation of *EGR1* gene products in the CA1 and DG regions of female α Syn-KO mice, regions known to play a critical role in long-term memory consolidation and retrieval (see [65] for review). Considering that spatial reference memory was impaired in female α Syn-KO mice and that electrophysiological recordings indicated a failure of female α Syn-KO mice to maintain LTP at CA1 SC synapses, these findings are in agreement with prior observations and indicate that sustained increased Egr1 may be deleterious for long-term memory.

Environmental interactions and neuronal activity are modulators of immediate early genes, such as *EGR1*. In turn, *ERGI* mediates many genes associated with neuronal signaling, protein translation and protein degradation [16]. While the results of our studies provide evidence for a novel connection between α Syn and Egr1, the molecular mechanism by which *SNCA* ablation impacts *EGR1* expression remains to be elucidated. However, our data unequivocally indicate that future studies should also carefully consider the effect of sex while investigating these mechanisms.

Conclusions

To conclude, the translational and genetic results presented here revealed a gender-specific responsiveness to murine ASO^{*SNCA*} and a novel sex-specific role of α Syn on learning and memory in mice. By extension, these findings suggest this new role for α Syn should be considered when developing any *SNCA* modulating therapy. Finally and more broadly, these observations underscore the fundamental importance of including both sexes in experimental groups when performing studies.

Abbreviations

AD	Alzheimer's disease
APP	J20 APP transgenic mice
ASO	Antisense oligonucleotide
A β	Amyloid-beta
BCM	Barnes circular maze
NTG	Non-transgenic mice
EGR1	Early growth response 1
WT	Wild-type
α Syn	Alpha-synuclein
α Syn-KO	SNCA-Null mice

Supplementary Information

The online version contains supplementary material available at <https://doi.org/10.1186/s40478-022-01480-y>.

Additional file 1: Summary table of statistical tests and outcomes.

Additional file 2: Supplementary figures.

Acknowledgements

We thank the University of Minnesota Genomics Center for their support and Dr. Ying Zhang for technical consultation.

Author contributions

JLB, GSB, DWH, TGB, ML, RP, SB, MK, MS, AB, and MAS performed experiments; JLB, SEL, GSB and MAS conceived, designed and supervised experiments. MKL provided reagents and critical feedback. JLB and SEL wrote the manuscript; JLB, GSB, DWH and SEL prepared and organized the figures. GSB, DWH, MK, ML, MAS, AA and MKL contributed to critical discussions and edited the manuscript. All authors read and approved the final manuscript.

Funding

This work was supported by grants from the National Institutes of Health (NIH) to SEL (RF1-AG044342, RF1-AG070296, R21-AG065693, R01-AG077743, R01-NS092918, R01-AG062135 and R56-NS113549), to MKL (AG062135, NS108686, NS086074, NS092093). Training grant support for graduate students (T32-NS105604). This study was supported by a grant from the Winston and Maxine Wallin Neuroscience Discovery Fund. Additional support included start-up funds from the University of Minnesota Foundation and bridge funds from the Institute of Translational Neuroscience to SEL.

Availability of data and materials

All data needed to evaluate the conclusions in the paper are present in the paper and the Supplementary Materials, Additional files 1 and 2. The data can be provided following scientific review and a completed material transfer agreement. Requests for data and materials should be submitted to the corresponding author.

Declarations**Ethics approval and consent to participate**

The University of Minnesota Institutional Review Board approved this study.

Consent for publication

All authors discussed the results, commented on this manuscript and gave approval for publication.

Competing interests

Unless stated subsequently, the authors declare that they have no competing interests. T. Cole: Other Research Support (receipt of drugs, supplies, equipment or other in-kind support); Provided drug (mouse alpha-synuclein ASO).

Received: 23 August 2022 Accepted: 18 November 2022

Published: 14 December 2022

References

- Abeliovich A, Schmitz Y, Fariñas I, Choi-Lundberg D, Ho WH, Castillo PE, Shinsky N, Garcia Verdugo JM, Armanini M, Ryan A, Hynes M, Phillips H, Sulzer D, Rosenthal A (2000) Mice lacking α -synuclein display functional deficits in the nigrostriatal dopamine system. *Neuron* 25:239–252. [https://doi.org/10.1016/S0896-6273\(00\)80886-7](https://doi.org/10.1016/S0896-6273(00)80886-7)
- Alarcón-Arís D, Pavia-Collado R, Miquel-Río L, Coppola-Segovia V, Ferrés-Coy A, Ruiz-Bronchal E, Galofré M, Paz V, Campa L, Revilla R, Montefeltro A, Kordower JH, Vila M, Artigas F, Bortolozzi A (2020) Anti- α -synuclein ASO delivered to monoamine neurons prevents α -synuclein accumulation in a Parkinson's disease-like mouse model and in monkeys. *EBioMedicine* 59:102944. <https://doi.org/10.1016/j.ebiom.2020.102944>
- Bachhuber T, Katzmarski N, McCarter JF, Loreth D, Tahirovic S, Kamp F, Abou-Ajram C, Nuscher B, Serrano-Pozo A, Müller A, Prinz M, Steiner H, Hyman BT, Haass C, Meyer-Luehmann M (2015) Inhibition of amyloid- β plaque formation by α -synuclein. *Nat Med* 21:802–807. <https://doi.org/10.1038/nm.3885>
- Bakalash S, Pham M, Koronyo Y, Salumbides BC, Kramerov A, Seidenberg H, Berel D, Black KL, Koronyo-Hamaoui M (2011) Egr1 expression is induced following glatiramer acetate immunotherapy in rodent models of glaucoma and alzheimer's disease. *Invest Ophthalmol Vis Sci* 52:9033–9046. <https://doi.org/10.1167/IOVS.11-7498>
- Bennett CF, Krainer AR, Cleveland DW (2019) Antisense oligonucleotide therapies for neurodegenerative diseases. *Annu Rev Neurosci* 42:385–406. <https://doi.org/10.1146/annurev-neuro-070918-050501>
- Bonow RH, Aid S, Zhang Y, Becker KG, Bosetti F (2009) The brain expression of genes involved in inflammatory response, the ribosome, and learning and memory is altered by centrally injected lipopolysaccharide in mice. *Pharmacogenomics J* 9:116–126. <https://doi.org/10.1038/tj.2008.15>
- Boutros SW, Raber J, Unni VK (2021) Effects of alpha-synuclein targeted antisense oligonucleotides on lewy body-like pathology and behavioral disturbances induced by injections of pre-formed fibrils in the mouse motor cortex. *J Parkinsons Dis* 11:1091–1115. <https://doi.org/10.3233/JPD-212566>
- Boyle PA, Yu L, Wilson RS, Leurgans SE, Schneider JA, Bennett DA (2018) Person-specific contribution of neuropathologies to cognitive loss in old age. *Ann Neurol* 83:74–83. <https://doi.org/10.1002/ana.25123>
- Cabin DE, Shimazu K, Murphy D, Cole NB, Gottschalk W, McIlwain KL, Orrison B, Chen A, Ellis CE, Paylor R, Lu B, Nussbaum RL (2002) Synaptic vesicle depletion correlates with attenuated synaptic responses to prolonged repetitive stimulation in mice lacking α -synuclein. *J Neurosci* 22:8797–8807. <https://doi.org/10.1523/jneurosci.22-20-08797.2002>
- Chandra S, Fornai F, Kwon HB, Yazdani U, Atasoy D, Liu X, Hammer RE, Battaglia G, German DC, Castillo PE, Südhof TC (2004) Double-knockout mice for α - and β -synucleins: effect on synaptic functions. *Proc Natl Acad Sci U S A* 101:14966–14971. <https://doi.org/10.1073/pnas.0406283101>
- Clinton LK, Blurton-Jones M, Myczek K, Trojanowski JQ, LaFerla FM (2010) Synergistic interactions between A β , tau, and α -synuclein: acceleration of neuropathology and cognitive decline. *J Neurosci* 30:7281–7289. <https://doi.org/10.1523/JNEUROSCI.0490-10.2010>
- Cole TA, Zhao H, Collier TJ, Sandoval I, Sortwell CE, Steece-Collier K, Daley BF, Booms A, Lipton J, Welch M, Berman M, Jandreski L, Graham D, Weihofen A, Celano S, Schulz E, Cole-Strauss A, Luna E, Quach D, Mohan A, Bennett CF, Swazy EE, Kordasiewicz HB, Luk KC, Paumier KL (2021) α -Synuclein antisense oligonucleotides as a disease-modifying therapy for Parkinson's disease. *JCI Insight*. <https://doi.org/10.1172/jci.insight.135633>

13. Davis AA, Inman CE, Wargel ZM, Dube U, Freeberg BM, Galluppi A, Haines JN, Dhavale DD, Miller R, Choudhury FA, Sullivan PM, Cruchaga C, Perlmutter JS, Ulrich JD, Benitez BA, Kotzbauer PT, Holtzman DM (2020) APOE genotype regulates pathology and disease progression in synucleinopathy. *Science Trans Med*. <https://doi.org/10.1126/scitranslmed.aay3069>
14. DeVos SL, Miller RL, Schoch KM, Holmes BB, Kebodeaux CS, Wegener AJ, Chen G, Shen T, Tran H, Nichols B, Zanardi TA, Kordasiewicz HB, Swayze EE, Bennett CF, Diamond MI, Miller TM (2017) Tau reduction prevents neuronal loss and reverses pathological tau deposition and seeding in mice with tauopathy. *Sci Transl Med*. <https://doi.org/10.1126/scitranslmed.aag0481>
15. Duclot F, Kabbaj M (2015) The estrous cycle surpasses sex differences in regulating the transcriptome in the rat medial prefrontal cortex and reveals an underlying role of early growth response 1. *Genome Biol* 16:1–20. <https://doi.org/10.1186/s13059-015-0815-x>
16. Duclot F, Kabbaj M (2017) The role of early growth response 1 (EGR1) in brain plasticity and neuropsychiatric disorders. *Front Behav Neurosci* 11:35
17. Friedrich J, Kordasiewicz HB, O'Callaghan B, Handler HP, Wagener C, Duvick L, Swayze EE, Rainwater O, Hofstra B, Benneyworth M, Nichols-Meade T, Yang P, Chen Z, Ortiz JP, Clark HB, Öz G, Larson S, Zoghbi HY, Henzler C, Orr HT (2018) Antisense oligonucleotide-mediated ataxin-1 reduction prolongs survival in SCA1 mice and reveals disease-associated transcriptome profiles. *JCI insight*. <https://doi.org/10.1172/jci.insight.123193>
18. Garthe A, Kempermann G (2013) An old test for new neurons: Refining the morris water maze to study the functional relevance of adult hippocampal neurogenesis. *Front Neurosci* 7:63
19. Gatta V, D'Aurora M, Granzotto A, Stuppia L, Sensi SL (2014) Early and sustained altered expression of aging-related genes in young 3xTg-AD mice. *Cell Death Dis* 5:e1054. <https://doi.org/10.1038/CDDIS.2014.11>
20. Gómez Ravetti M, Rosso OA, Berretta R, Moscato P (2010) Uncovering molecular biomarkers that correlate cognitive decline with the changes of hippocampus' gene expression profiles in alzheimer's disease. *PLoS One* 5:e10153. <https://doi.org/10.1371/JOURNAL.PONE.0010153>
21. Gonzalez MC, Rossato JI, Radiske A, Pádua Reis M, Cammarota M (2019) Recognition memory reconsolidation requires hippocampal Zif268. *Sci Rep*. <https://doi.org/10.1038/s41598-019-53005-8>
22. Jankowsky JL, Zheng H (2017) Practical considerations for choosing a mouse model of Alzheimer's disease. *Mol Neurodegener* 12(1):1–22
23. Johnson ECB, Ho K, Yu GQ, Das M, Sanchez PE, Djukic B, Lopez I, Yu X, Gill M, Zhang W, Paz JT, Palop JJ, Mucke L (2020) Behavioral and neural network abnormalities in human APP transgenic mice resemble those of App knock-in mice and are modulated by familial Alzheimer's disease mutations but not by inhibition of BACE1. *Mol Neurodegener* 15:53. <https://doi.org/10.1186/s13024-020-00393-5>
24. Jones MW, Errington ML, French PJ, Fine A, Bliss TVP, Garel S, Charnay P, Bozon B, Laroche S, Davis S (2001) A requirement for the immediate early gene Zif268 in the expression of late LTP and long-term memories. *Nat Neurosci* 4(4):289–296. <https://doi.org/10.1038/85138>
25. Khan SS, LaCroix M, Boyle G, Sherman MA, Brown JL, Amar F, Aldaco J, Lee MK, Bloom GS, Lesné SE (2018) Bidirectional modulation of Alzheimer phenotype by alpha-synuclein in mice and primary neurons. *Acta Neuropathol* 136:589–605. <https://doi.org/10.1007/s00401-018-1886-z>
26. Killick R, Ribe EM, Al-Shawi R, Malik B, Hooper C, Fernandes C, Dobson R, Nolan PM, Louridasamy A, Furney S, Lin K, Breen G, Wroe R, To AWM, Leroy K, Causevic M, Usardi A, Robinson M, Noble W, Williamson R, Lunnon K, Kellie S, Reynolds CH, Bazenet C, Hodges A, Brion JP, Stephenson J, Paul Simons J, Lovestone S (2014) Clusterin regulates β -amyloid toxicity via Dickkopf-1-driven induction of the wnt–PCP–JNK pathway. *Mol Psychiatry* 19:88. <https://doi.org/10.1038/MP2012.163>
27. Kole R, Krainer AR, Altman S (2012) RNA therapeutics: beyond RNA interference and antisense oligonucleotides. *Nat Rev Drug Discov* 11:125–140
28. Komaki H, Nagata T, Saito T, Masuda S, Takeshita E, Sasaki M, Tachimori H, Nakamura H, Aoki Y, Takeda S (2018) Systemic administration of the antisense oligonucleotide NS-065/NCNP-01 for skipping of exon 53 in patients with Duchenne muscular dystrophy. *Sci Transl Med*. <https://doi.org/10.1126/scitranslmed.aan0713>
29. Larson ME, Greimel SJ, Amar F, LaCroix M, Boyle G, Sherman MA, Schley H, Miel C, Schneider JA, Kaye R, Benfenati F, Lee MK, Bennett DA, Lesné SE (2017) Selective lowering of synapsins induced by oligomeric α -synuclein exacerbates memory deficits. *Proc Natl Acad Sci USA* 114:E4648–E4657. <https://doi.org/10.1073/pnas.1704698114>
30. Larson ME, Sherman MA, Greimel S, Kuskowski M, Schneider JA, Bennett DA, Lesné SE (2012) Soluble α -synuclein is a novel modulator of Alzheimer's disease pathophysiology. *J Neurosci* 32:10253–10266. <https://doi.org/10.1523/JNEUROSCI.0581-12.2012>
31. Lee J, Pinares-Garcia P, Loke H, Ham S, Vilain E, Harley VR (2019) Sex-specific neuroprotection by inhibition of the Y-chromosome gene, SRY, in experimental Parkinson's disease. *Proc Natl Acad Sci USA* 116:16577–16582. <https://doi.org/10.1073/pnas.1900406116>
32. Lesné S, Ming TK, Kotilinek L, Kaye R, Glabe CG, Yang A, Gallagher M, Ashe KH (2006) A specific amyloid- β protein assembly in the brain impairs memory. *Nature* 440:352–357. <https://doi.org/10.1038/nature04533>
33. Lu Y, Li T, Qureshi HY, Han D, Paudel HK (2011) Early growth response 1 (Egr-1) regulates phosphorylation of microtubule-associated protein tau in mammalian brain. *J Biol Chem* 286:20569–20581. <https://doi.org/10.1074/jbc.M111.220962>
34. MacGibbon GA, Lawlor PA, Walton M, Sirimanne E, Faul RLM, Synek B, Mee E, Connor B, Dragunow M (1997) Expression of Fos, Jun, and Krox family proteins in Alzheimer's disease. *Exp Neurol* 147:316–332. <https://doi.org/10.1006/EXNR.1997.6600>
35. Masliah E, Rockenstein E, Veinbergs I, Sagar Y, Mallory M, Hashimoto M, Mucke L (2001) β -Amyloid peptides enhance α -synuclein accumulation and neuronal deficits in a transgenic mouse model linking Alzheimer's disease and Parkinson's disease. *Proc Natl Acad Sci U S A* 98:12245–12250. <https://doi.org/10.1073/pnas.211412398>
36. Mercuri E, Darras BT, Chiriboga CA, Day JW, Campbell C, Connolly AM, Iannaccone ST, Kirschner J, Kuntz NL, Saito K, Shieh PB, Tulinius M, Mazzone ES, Montes J, Bishop KM, Yang Q, Foster R, Gheuens S, Bennett CF, Farwell W, Schneider E, De Vivo DC, Finkel RS (2018) Nusinersen versus sham control in later-onset spinal muscular atrophy. *N Engl J Med* 378:625–635. <https://doi.org/10.1056/NEJMoa1710504>
37. Miguel-Aliaga I (2022) Let's talk about (biological) sex. *Nat Rev Mol Cell Biol* 23:227–228
38. Moussaud S, Jones DR, Moussaud-Lamodière EL, Delenclos M, Ross OA, McLean PJ (2014) Alpha-synuclein and tau: teammates in neurodegeneration? *Mol Neurodegener* 9:43
39. Mucke L, Masliah E, Yu GQ, Mallory M, Rockenstein EM, Tatsuno G, Hu K, Kholodenko D, Johnson-Wood K, McConlogue L (2000) High-level neuronal expression of A β (1–42) in wild-type human amyloid protein precursor transgenic mice: synaptotoxicity without plaque formation. *J Neurosci* 20:4050–4058. <https://doi.org/10.1523/JNEUROSCI.20-11-04050.2000>
40. Norambuena A, Wallrabe H, McMahon L, Silva A, Swanson E, Khan SS, Baerthlein D, Kodis E, Oddo S, Mandell JW, Bloom GS (2017) mTOR and neuronal cell cycle reentry: How impaired brain insulin signaling promotes Alzheimer's disease. *Alzheimer's Dement* 13:152–167. <https://doi.org/10.1016/j.jalz.2016.08.015>
41. Passini MA, Bu J, Richards AM, Kinnecom C, Sardi SP, Stanek LM, Hua Y, Rigo F, Matson J, Hung G, Kaye EM, Shihabuddin LS, Krainer AR, Bennett CF, Cheng SH (2011) Antisense oligonucleotides delivered to the mouse CNS ameliorate symptoms of severe spinal muscular atrophy. *Sci Trans Med*. <https://doi.org/10.1126/scitranslmed.3001777>
42. Pavia-Collado R, Còppola-Segovia V, Miquel-Rio L, Alarcón-Aris D, Rodríguez-Aller R, Torres-López M, Paz V, Ruiz-Bronchal E, Campa L, Artigas F, Montefeltro A, Revilla R, Bortolozzi A (2021) Intracerebral administration of a ligand-asso conjugate selectively reduces α -synuclein accumulation in monoamine neurons of double mutant human a30p*A53t* α -synuclein transgenic mice. *Int J Mol Sci* 22:1–20. <https://doi.org/10.3390/ijms22062939>
43. Penke Z, Morice E, Veyrac A, Gros A, Chagneau C, LeBlanc P, Samson N, Baumgärtel K, Mansuy IM, Davis S, Laroche S (2014) Zif268/Egr1 gain of function facilitates hippocampal synaptic plasticity and long-term spatial recognition memory. *Philos Trans R Soc B Biol Sci*. <https://doi.org/10.1098/RSTB.2013.0159>
44. Pollak DD, Scharl T, Leisch F, Herkner K, Villar SR, Hoeger H, Lubec G (2005) Strain-dependent regulation of plasticity-related proteins in the mouse hippocampus. *Behav Brain Res* 165:240–246. <https://doi.org/10.1016/j.bbr.2005.07.028>

45. Przybyla M, Van Eersel J, Van Hummel A, Van Der Hoven J, Sabale M, Harasta A, Mü J, Gajwani M, Prikas E, Mueller T, Stevens CH, Power J, Housley GD, Karl T, Kassiou M, Ke YD, Ittner A, Ittner LM (2020) Onset of hippocampal network aberration and memory deficits in P301S tau mice are associated with an early gene signature. *Brain*. <https://doi.org/10.1093/brain/awaa133>
46. Qin X, Wang Y, Paudel HK (2017) Inhibition of early growth response 1 in the hippocampus alleviates neuropathology and improves cognition in an Alzheimer model with plaques and tangles. *Am J Pathol* 187:1828–1847. <https://doi.org/10.1016/j.ajpath.2017.04.018>
47. Rinaldi C, Wood MJA (2018) Antisense oligonucleotides: the next frontier for treatment of neurological disorders. *Nat Rev Neurol* 14:9–22
48. Robinson JL, Lee EB, Xie SX, Rennett L, Suh E, Bredenberg C, Caswell C, Van Deerlin VM, Yan N, Yousef A, Hurtig HI, Siderowf A, Grossman M, McMillan CT, Miller B, Duda JE, Irwin DJ, Wolk D, Elman L, McCluskey L, Chen-Plotkin A, Weintraub D, Arnold SE, Brettschneider J, Lee VMY, Trojanowski JQ (2018) Neurodegenerative disease concomitant proteinopathies are prevalent, age-related and APOE4-associated. *Brain* 141:2181–2193. <https://doi.org/10.1093/brain/awy146>
49. Rockenstein E, Hansen LA, Mallory M, Trojanowski JQ, Galasko D, Masliah E (2001) Altered expression of the synuclein family mRNA in Lewy body and Alzheimer's disease. *Brain Res* 914:48–56. [https://doi.org/10.1016/S0006-8993\(01\)02772-X](https://doi.org/10.1016/S0006-8993(01)02772-X)
50. Saito T, Matsuba Y, Mihira N, Takano J, Nilsson P, Itohara S, Iwata N, Saido TC (2014) Single App knock-in mouse models of Alzheimer's disease. *Nat Neurosci* 17:661–663. <https://doi.org/10.1038/nn.3697>
51. Schindelin J, Arganda-Carreras I, Frise E, Kaynig V, Longair M, Pietzsch T, Preibisch S, Rueden C, Saalfeld S, Schmid B, Tinevez JY, White DJ, Hartenstein V, Eliceiri K, Tomancak P, Cardona A (2012) Fiji: an open-source platform for biological-image analysis. *Nat Methods* 9(9):676–682. <https://doi.org/10.1038/nmeth.2019>
52. Schneider JA, Aggarwal NT, Barnes L, Boyle P, Bennett DA (2009) The neuropathology of older persons with and without dementia from community versus clinic cohorts. *J Alzheimer's Dis* 18:691–701. <https://doi.org/10.3233/JAD-2009-1227>
53. Scholz B, Doidge AN, Barnes P, Hall J, Wilkinson LS, Thomas KL (2016) The regulation of cytokine networks in hippocampal CA1 differentiates extinction from those required for the maintenance of contextual fear memory after recall. *PLoS One* 11:e0153102. <https://doi.org/10.1371/JOURNAL.PONE.0153102>
54. Seward ME, Swanson E, Norambuena A, Reimann A, Nicholas Cochran J, Li R, Roberson ED, Bloom GS (2013) Amyloid- β signals through tau to drive ectopic neuronal cell cycle re-entry in Alzheimer's disease. *J Cell Sci* 126:1278–1286. <https://doi.org/10.1242/jcs.1125880>
55. Shannon P, Markiel A, Ozier O, Baliga NS, Wang JT, Ramage D, Amin N, Schwikowski B, Ideker T (2003) Cytoscape: a software environment for integrated models of biomolecular interaction networks. *Genome Res* 13:2498. <https://doi.org/10.1101/GR.1239303>
56. Spencer B, Desplats PA, Overk CR, Valera-Martin E, Rissman RA, Wu C, Mante M, Adame A, Florio J, Rockenstein E, Masliah E (2016) Reducing endogenous α -synuclein mitigates the degeneration of selective neuronal populations in an Alzheimer's disease transgenic mouse model. *J Neurosci* 36:7971–7984. <https://doi.org/10.1523/JNEUROSCI.0775-16.2016>
57. Stack A, Carrier N, Dietz D, Hollis F, Sorenson J, Kabbaj M (2010) Sex differences in social interaction in rats: role of the immediate-early gene zif268. *Neuropsychopharmacology* 35:570–580. <https://doi.org/10.1038/npp.2009.163>
58. Uehara T, Choong CJ, Nakamori M, Hayakawa H, Nishiyama K, Kasahara Y, Baba K, Nagata T, Yokota T, Tsuda H, Obika S (2019) Mochizuki H (2019) Amido-bridged nucleic acid (AmNA)-modified antisense oligonucleotides targeting α -synuclein as a novel therapy for Parkinson's disease. *Sci Reports* 9(1):1–13. <https://doi.org/10.1038/s41598-019-43772-9>
59. Vegeto E, Villa A, Della Torre S, Crippa V, Rusmini P, Cristofani R, Galbiati M, Maggi A, Poletti A (2019) The role of sex and sex hormones in neurodegenerative diseases. *Endocr Rev* 41(2):273–319
60. Veyrac A, Besnard A, Caboche J, Davis S, Laroche S (2014) The transcription factor Zif268/Egr1, brain plasticity, and memory. *Prog Mol Biol Transl Sci* 122:89–129. <https://doi.org/10.1016/B978-0-12-420170-5.00004-0>
61. Veyrac A, Besnard A, Caboche J, Davis S, Laroche S (2014) The transcription factor Zif268/Egr1, brain plasticity, and memory. In: *Progress in Molecular Biology and Translational Science*. pp 89–129
62. Wright AL, Zinn R, Hohensinn B, Konen LM, Beynon SB, Tan RP, Clark IA, Abdipranoto A, Vissel B (2013) Neuroinflammation and neuronal loss precede A β plaque deposition in the hAPP-J20 mouse model of Alzheimer's disease. *PLoS One* 8:e59586. <https://doi.org/10.1371/journal.pone.0059586>
63. Yang J, Luo S, Zhang J, Yu T, Fu Z, Zheng Y, Xu X, Liu C, Fan M, Zhang Z (2021) Exosome-mediated delivery of antisense oligonucleotides targeting α -synuclein ameliorates the pathology in a mouse model of Parkinson's disease. *Neurobiol Dis* 148:105218. <https://doi.org/10.1016/j.NBD.2020.105218>
64. Yu J, de Belle I, Liang H, Adamson ED (2004) Coactivating factors p300 and CBP are transcriptionally crossregulated by Egr1 in prostate cells, leading to divergent responses. *Mol Cell* 15:83–94. <https://doi.org/10.1016/j.molcel.2004.06.030>
65. Zemla R, Basu J (2017) Hippocampal function in rodents. *Curr Opin Neurobiol* 43:187–197

Publisher's Note

Springer Nature remains neutral with regard to jurisdictional claims in published maps and institutional affiliations.